Interaction Notes

Note 102

April 1972

# On the Singularity Expansion Method as Applied to Electromagnetic Scattering from Thin-Wires

by

F. M. Tesche
The Dikewood Corp.
Albuquerque, New Mexico

## Abstract

In this note, the possibility of analyzing scattering and antenna problems from a singularity expansion point of view is discussed. As an example of the method, a thin-wire scatterer is considered by first determining the locations of the exterior natural resonant frequencies and then constructing the time response of the current on the body, much in the same manner as in classical circuit theory. The numerical techniques used will be presented, and some advantages of the natural resonance method over the other conventional ways of treating this problem will be mentioned.

Interaction Notes

Note 102

April 1972

# On the Singularity Expansion Method as Applied to Electromagnetic Scattering from Thin-Wires

by

F. M. Tesche
The Dikewood Corp.
Albuquerque, New Mexico

## Abstract

In this note, the possibility of analyzing scattering and antenna problems from a singularity expansion point of view is discussed. As an example of the method, a thin-wire scatterer is considered by first determining the locations of the exterior natural resonant frequencies and then constructing the time response of the current on the body, much in the same manner as in classical circuit theory. The numerical techniques used will be presented, and some advantages of the natural resonance method over the other conventional ways of treating this problem will be mentioned.

## Acknowledgements

I would like to thank Dr. Carl Baum for his initial ideas regarding this work, and for his many valuable suggestions. In addition, thanks go to Drs. Kelvin Lee, Ray Latham and Lennart Marin at Northrop for their discussions during the course of this work.

## I. Introduction

In classical circuit theory, the description of the time domain response of a linear circuit which is excited by an arbitrary waveform may be determined by knowledge of the location of any singularities of the response function in the complex frequency plane, as well as the corresponding residues. The time domain behavior of circuit may be obtained as a sum of all of the residues multiplied by exponentially damped sinusoids. The purpose of this paper is to verify the extension of this method to electromagnetic scattering and antenna problems.

In the past, the time domain response of an electromagnetic scattering body has been determined either by time harmonic analysis coupled with Fourier inversion, or by direct time domain solution. For a change in the angle of incidence, the polarization, or the time behavior of the incident wave, considerable effort must be spent to recalculate the scattering behavior of the obstacle. As will be evident in the next section, the natural frequency method provides a means of rapidly computing the response of the scatterer or antenna for a wide variety of parameters.

A number of early investigators have treated the exterior natural resonance problem to some degree. Pocklington[9] developed an approximate relation for finding the natural resonances of a linear and a circular ring scatterer. The case of a prolate spheroid and later the limiting case of a thin-wire has been investigated by Page and Adams[8] and the case of a spherical scatterer is treated by Stratton.[10]

More recently, Baum[1] formalized the singularity expansion technique as applied to general scattering problems by defining the natural frequencies, modes, and coupling coefficients which arise for a general three dimensional body. Marin and Latham[6] have investigated some of the analytical properties of the scattered field from a perfectly conducting, finite body and approximate natural resonance frequencies of a thin cylinder have been obtained by Lee and Leung.[5]

The present note is a logical extension of this previous work. From the E-field integral equation for currents on a thin-wire scatterer, the method of moments is employed to form a matrix equation. The zeros of the determinant of the system matrix define the locations of the natural resonance, and are found by a numerical search procedure. At each of the natural resonances, it is possible to define a matrix of residues, from which the time domain response of the structure can be computed in terms of exponentially damped sinusoids. The residue matrix is a dyadic and can be defined by two N-dimensional vectors and, in the E-field formulation, these vectors are identical. Moreover, these vectors are independent of the angle of incidence of the incoming wave. As a result, the scattering body may be characterized by a few pole locations with the corresponding vectors, and the solution for any wave incident obtained.

As will be shown, this method is more rapid than the conventional frequency domain, Fourier transform technique. For late times, $ct/L > 3$, only about 3 or 4 poles are needed to adequately describe the time behavior of the currents for an incident step wave which grazes the axis of the scatterer. For broadside incidence, even fewer poles are needed.

It should be pointed out that in the sections to follow, only the scattering case is considered. The application of this method to the antenna problem is straightforward, requiring only a modification of the excitation function so that it is non-zero only over a finite gap on the wire structure.

## II. Formulation

Consider a thin-wire scattering element of length L and diameter d which is struck by an incident pulse of electromagnetic radiation. As shown in Figure 1, the incident electric field is assumed to lie in the plane of the figure and the direction of propagation makes an angle $\theta$ with the axis of the wire. For convenience, it is assumed that the time behavior of the incident wave is described by a step function, striking the scattering wire of $z = 0$ at time $t = 0$. It is then desired to obtain the induced currents and charges on the wire as a function of time.

Neglecting the effect of the end-caps on the wire, a Pocklington type integro-differential equation can be written for the axially directed current flowing on the wire.[7] Using the complex frequency $s = j\omega + \sigma$ and assuming that the temporal variation of the fields goes as $e^{st}$, this equation takes the form

$$-s\varepsilon_o E^{inc}(z,s) = \int_o^L I(z',s)\left(\frac{\partial^2}{\partial z^2} - \frac{s^2}{c^2}\right)K(z,z',s)\,dz' \qquad (1)$$

where the kernel K is given by

$$K(z,z',s) = \frac{1}{2\pi a}\int_o^{2\pi} \frac{e^{-sR/c}}{4\pi R}\,a\,d\phi \qquad (2)$$

with $$R = [(z-z')^2 + d^2\sin^2(\phi/2)]^{1/2} . \qquad (3)$$

This kernel is exact in the sense that the thin-wire approximation is not used.

The incident tangential electric field along the wire is given by

$$E^{inc}(z,s) = E_o(s)\sin\theta\, e^{-sz\cos\theta/c} \qquad (4)$$

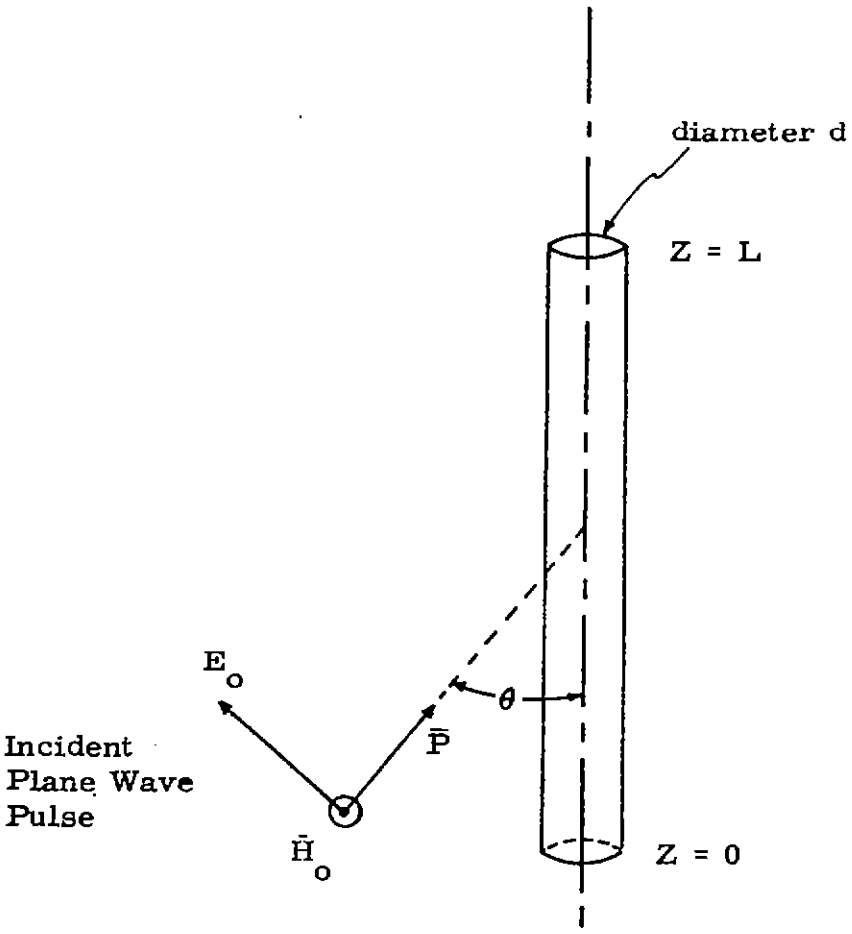


Figure 1. Geometry of the wire scatterer and incident field.

and for a step wave,

$$E_o(s) = E_o/s \ . \tag{5}$$

From knowledge of the current on the wire, the linear charge density, $\rho$, can be obtained from the equation of continuity

$$\frac{dI(z,s)}{dz} = -s\rho(z,s) \ . \tag{6}$$

In order to find the time domain behavior of the wire current, it is customary to solve Eq. (1) for a large number of frequencies along the contour $s = j\omega$, and then numerically perform a Fourier inversion. The method of moments may be employed to obtain the solution for $I(z,j\omega)$ and the Fast Fourier Transform algorithm[2,3] is one possible way to obtain the inverse Fourier transform.

A typical plot showing the magnitudes of the currents in the frequency domain as observed at $z = .25L$, $.50L$, and $.75L$ on a thin wire with $d/L = .01$ is shown in Figure 2. For these particular curves, the angle of incidence is $\theta = 30°$ and it is assumed that $E_o(s)$ is a constant. Hence, this spectrum is that resulting from an impulsive incident field, not an incident step. The corresponding spectrum for the step wave is then obtained by a multiplication by $(kL)^{-1}$.

The resonance-like behavior of the currents as the frequency increases suggests that there are singular points in the response at certain points just off of the $j\omega$ axis in the complex s plane, much in the same manner as in classical circuit theory. This fact has been verified for the sphere[1,10] and prolate spheroid[8] and has been postulated as true for any finite scattering body.[1] That the response function for bodies of finite extent has only poles and no branch cuts has been shown by Marin[6], and it is speculated, but not rigorously proved, that these poles are simple for perfectly conducting bodies.

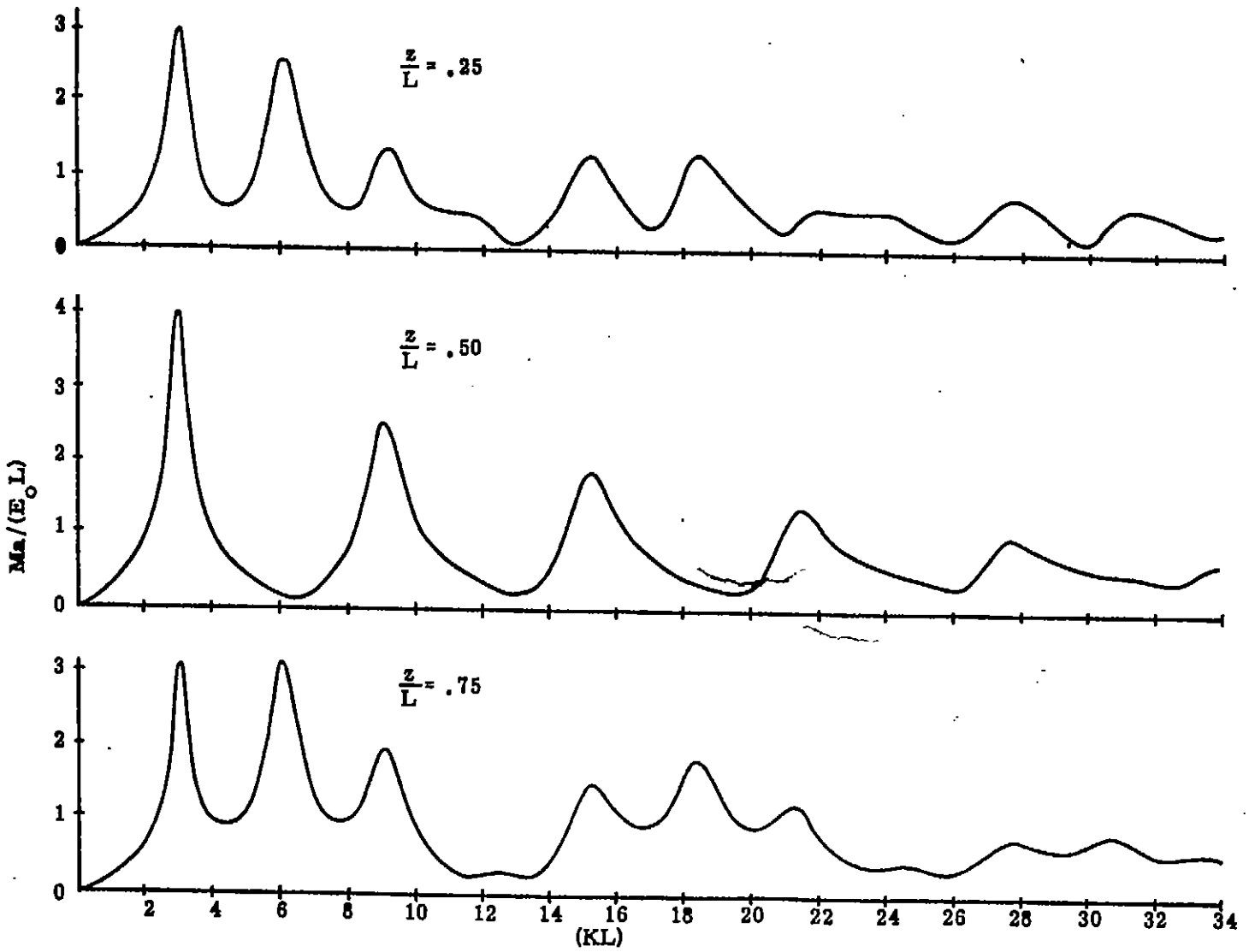


Figure 2. Plots of the magnitude of the induced current at $z/L = .25, .50,$ and $.75$ on a scattering wire with $d/L = .01$, as determined from the integral equation solution.

To study the thin-wire scattering or antenna problem from this point of view, it is first necessary to determine the location of any poles of the current function $I(z,s)$ in the complex s plane. This is equivalent to finding the frequencies at which there can exist a non-trivial solution of Eq. (1) with $E^{inc} = 0$.

Eq. (1) may be cast into matrix form by the application of the method of moments as described by Harrington.[4] The result is of the form

$$\overline{\overline{[Z(s)]}}\,\overline{[I(s)]} = \overline{[V(s)]} \tag{7}$$

where $\overline{\overline{[Z(s)]}}$ is an n×n matrix and is referred to as the system impedance matrix. $\overline{[I]}$ and $\overline{[V]}$ are the response and source vectors respectively, and are of dimension n.

The natural frequencies of the thin-wire, denoted by $s_\alpha$, are those such that the homogeneous version of Eq. (7)

$$\overline{\overline{[Z(s_\alpha)]}}\,\overline{[I(s_\alpha)]} = 0 \tag{8}$$

has a non-trivial solution for $\overline{[I]}$. The implication of this is that the determinant of $\overline{\overline{[Z]}}$ must vanish at these frequencies. Hence, the equation for determining the natural resonances of the current becomes

$$\det\overline{\overline{[Z(s_\alpha)]}} \equiv \Delta(s_\alpha) = 0 \tag{9}$$

From the circuit theory analogy, a number of things can be inferred regarding the location and nature of the natural resonances. These resonances must occur in the left-hand portion of the s plane since the time behavior is as $e^{st}$ and exponentially growing currents are now allowed. Moreover, the poles must occur

which contribute to the time behavior must not reside on the jω axis. It is assumed, but without proof, that the poles are all simple. This has been substantiated numerically.

The solution to Eq. (7) can be written in the form

$$[\overline{I(s)}] = \frac{\overline{\overline{[Y(s)]}}}{\Delta(s)} [\overline{V(s)}] \tag{10}$$

where $[\overline{\overline{Z(s)}}]^{-1} \equiv \frac{\overline{\overline{[Y(s)]}}}{\Delta(s)}$ so as to show the dependence on $\Delta$ explicitly. The construction of the time domain response is then given as

$$[\overline{i(t)}] = \frac{1}{2\pi j} \int_{\sigma_o - j\infty}^{\sigma_o + j\infty} \frac{\overline{\overline{[Y(s)]}}}{\Delta(s)} [\overline{V(s)}] e^{st} ds \ . \tag{11}$$

Instead of numerically evaluating this integral along the $\sigma_o$ contour, it is possible to apply the residue theorem to find the time response. Assume for the moment that $[\overline{\overline{Z}}]^{-1}$ can be represented as

$$[\overline{\overline{Z(s)}}]^{-1} = \frac{\overline{\overline{[Y(s)]}}}{\Delta(s)} = \sum_{\alpha} \frac{\overline{\overline{[R_\alpha]}}}{s - s_\alpha} \tag{12}$$

which is a sum over all of the poles in the complex s plane. The constant matrix $\overline{\overline{[R_\alpha]}}$ is referred to as the system residue matrix at the pole at $s_\alpha$. It has been shown by Marin and Latham[6] and by Baum[1] that this residue matrix is actually a dyadic and can be represented as the outer product of two n dimensional vectors independent of s as

$$\overline{\overline{[R_\alpha]}} = [\overline{M_\alpha}] [\overline{C_\alpha}]^T \ . \tag{13}$$

Here $\overline{[M_\alpha]}$ is defined as the natural mode vector and is a solution to the equation

$$\overline{\overline{[Z(s_\alpha)]}}\,\overline{[M_\alpha]} = 0 \ . \tag{14}$$

The vector $\overline{[C_\alpha]}$ is referred to as the coupling vector, and solves the equation

$$\overline{\overline{[Z(s_\alpha)]}}^{T}\,\overline{[C_\alpha]} = 0 \tag{15}$$

where the T denotes the transpose. For the electric field formulation where symmetric matrices are encountered, the coupling vectors and the natural mode vectors are the same, so that the residue matrix becomes

$$\overline{\overline{[R_\alpha]}} = \overline{[C_\alpha]}\,\overline{[C_\alpha]}^{T} \ , \tag{16}$$

where $\overline{[C_\alpha]}^{T}$ is the transpose of $\overline{[C_\alpha]}$.

It should be pointed out that the expansion of $\overline{\overline{[Z]}}^{-1}$ in Eq. (12) is incapable of representing any essential singularity which may occur in the complex s plane at infinity. The matrix $\overline{\overline{[Y(s)]}}$ of Eq. (12) involves terms like $e^{s\tau}$ which show a singular behavior as $s \to \infty$. For the present analysis, this inadequacy is neglected and only the effects of the poles in the finite s plane will be considered. As numerical results will show later, the effects of such singularities at infinity are not important in the time domain solution for this particular example.

With such a representation for $\overline{\overline{[Z]}}^{-1}$, Eq. (11) becomes

$$\overline{[i(t)]} = \frac{1}{2\pi j}\int_{\sigma_o-j\infty}^{\sigma_o+j\infty}\sum_{\alpha}\frac{\overline{[C_\alpha]}\,\overline{[C_\alpha]}^{T}}{(s - s_\alpha)}\,\overline{[V(s)]}\ e^{st}ds \ . \tag{17}$$

The forcing vector $\overline{[V(s)]}$ also can have poles in the finite s plane. For example, the step wave excitation has a single pole at s = 0. Indicating this pole explicitly as

$$\overline{[V(s)]} = \frac{\overline{[V_o(s)]}}{s} , \tag{18}$$

Eq. (17) can be written as

$$\overline{[i(t)]} = \frac{1}{2\pi j}\int_{\sigma_o - j\infty}^{\sigma_o + j\infty} \sum_{\alpha} \left( \frac{\overline{[C_\alpha]}\overline{[C_\alpha]}^T \overline{[V_o(s)]}}{s_\alpha (s - s_\alpha)} e^{st} - \frac{\overline{[C_\alpha]}\,\overline{[C_\alpha]}^T \overline{[V_o(s)]} e^{st}}{s\, s_\alpha} \right) ds \tag{19}$$

The first term of this equation contains the singularities of the thin-wire scatterer, while the second term contains the singularities of the incident waveform. For a more general type of incident electromagnetic pulse, there might be poles other than the one at s = 0 for this last term.

Interchanging the order of summation and integration in Eq. (19) yields the following equation:

$$\overline{[i(t)]} = \frac{1}{2\pi j} \sum_{\alpha} \left\{ \int_{\sigma_o - j\infty}^{\sigma_o + j\infty} \frac{\overline{[C_\alpha]}\,\overline{[C_\alpha]}^T}{(s - s_\alpha)} \frac{\overline{[V_o(s)]}}{s_\alpha} e^{st} ds \right.$$

$$\left. - \int_{\sigma_o - j\infty}^{\sigma_o + j\infty} \frac{\overline{[C_\alpha]}\,\overline{[C_\alpha]}^T}{s_\alpha} \frac{\overline{[V_o(s)]}}{s} e^{st} ds \right\} \tag{20}$$

Closing the contour along $j\omega = \sigma_o$ at $\infty$ in either the left-hand or right-hand part of the complex s plane will permit the evaluation of the integrals in the previous equation by the Cauchy residue theorem. Thus,

$$\oint_{C=C_\infty+C_\sigma} \frac{\overline{[C_\alpha]}\,\overline{[C_\alpha]}^T}{(s - s_\alpha)} \frac{\overline{[V_o(s)]}}{s_\alpha} e^{st} ds = (2\pi j)\,\overline{[C_\alpha]}\,\overline{[C_\alpha]}^T \frac{\overline{[V_o(s_\alpha)]}}{s_\alpha} \overline{\overline{[U(t)]}} e^{s_\alpha t} \tag{21}$$

$$\text{and } \oint_{C=C_\infty+C_\sigma} \frac{\overline{[C_\alpha]}\,\overline{[C_\alpha]}^T}{s_\alpha} \frac{\overline{[V_o(s)]}}{s} e^{st} ds = (2\pi j) \frac{\overline{[C_\alpha]}\,\overline{[C_\alpha]}^T}{s_\alpha} \overline{[V_o(0)]}\,\overline{\overline{[U(t)]}} \tag{22}$$

In Eq. (21) $\overline{\overline{[U(t)]}}$ is a diagonal matrix of unit Heaviside functions which serves to enforce the requirements of causality. That this Heaviside matrix is necessary can be seen from the following. Suppose we consider the contribution to the current in the $i^{th}$ cell or zone on the scatterer due to the incident wave falling on the $k^{th}$ cell having length $(\Delta z_k)$. This fraction of the total response can be written from Eq. (21) as

$$\oint_C \frac{(C_\alpha)_i (C_\alpha)_k}{(s - s_\alpha)} \frac{(V_o(s))_k}{s} e^{st} ds = 2\pi j (C_\alpha)_i (C_\alpha)_k \frac{(V_o(s_\alpha))_k}{s_\alpha} U(t)_{kk} e^{s_\alpha t} \tag{23}$$

where

$$(V_o(s_\alpha))_k = E_o \sin\theta (\Delta z_k)\, e^{-s_\alpha z_k \cos\theta/c} .$$

Defining $t_k = z_k \cos\theta/c$, it is seen that the exponential function in Eq. (23) becomes $e^{s_\alpha(t-t_k)}$. From the shifting theorem, this implies that for $t < t_k$ the contour $C_\infty$ is to be closed in the right-hand part of the complex s plane, giving no contribution to the integral. For $t > t_k$, there is a contribution given by Eq. (21). Hence, $U_{kk}(t) = U(t - z_k \cos\theta/c)$.

A graphical representation of this effect is shown in Figure 3. Suppose the incident wave strikes the wire at z = 0 at t = 0

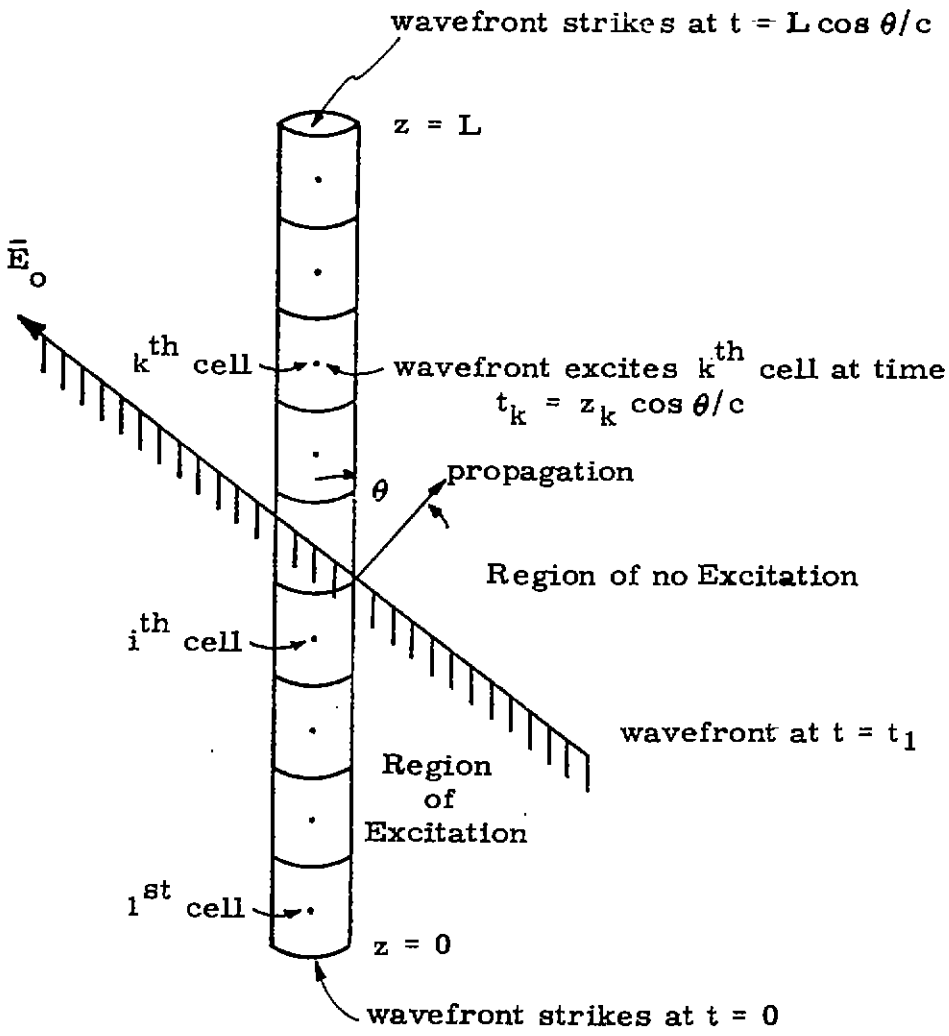


Figure 3. Diagram showing the relation between the incident field and the scattering wire in early times.

and at time $t_1$, it is desired to calculate the induced current at some point on the structure. If $t_1$ is such that the incident wave has not yet propagated completely across the wire, only those cells which are excited by the field will contribute to the integral in Eq. (19). After the wave front has completely passed by the obstacle, each cell contributes to the current and the Heaviside matrix becomes the identity matrix.

Inserting Eqs. (21) and (22) into Eq. (20) and noting that the integral on $C_\infty$ of the simple pole terms is zero, the following equation for the current results:

$$\overline{[i(t)]} = \sum_\alpha \overline{[C_\alpha]}\,\overline{[C_\alpha]}^T \frac{\overline{[V_o(s_\alpha)]}}{s_\alpha} \overline{\overline{[U(t)]}} e^{s_\alpha t} - \sum_\alpha \frac{\overline{[C_\alpha]}\overline{[C_\alpha]}^T}{s_\alpha} \overline{[V_o(0)]}\overline{\overline{[U(t)]}} \tag{24}$$

The last term must sum to zero, since it is constant in time, and the axial current on the antenna must approach zero for late time. Thus, the time domain solution for the current on the wire becomes

$$\overline{[i(t)]} = \sum_\alpha \overline{[C_\alpha]}\,\overline{[C_\alpha]}^T \frac{\overline{[V_o(s_\alpha)]}}{s_\alpha} \overline{\overline{[U(t)]}} e^{s_\alpha t} \,. \tag{25}$$

For late times such that the Heaviside matrix is a unit matrix, this expression is simply a sum of damped sinusoids.

A corresponding equation for the linear charge density along the wire can be developed. Starting with Eq. (17) and using the continuity equation, we have

$$\overline{[\rho(t)]} = \frac{-1}{2\pi j} \int_{\sigma_o - j\infty}^{\sigma_o + j\infty} \sum_\alpha \frac{\overline{[D_\alpha]}\,\overline{[C_\alpha]}^T}{s(s - s_\alpha)} \overline{[V_o(s)]} e^{st} ds \,, \tag{26}$$

where the 1/s dependence of $\overline{[V(s)]}$ has been shown explicitly, and the vector $\overline{[D_\alpha]}$ is the discrete representation of the $\alpha^{th}$ natural mode for the charge and it is determined by

$$D_\alpha(z) = \frac{d}{dz} C_\alpha(z) \tag{27}$$

Note that in this expression that there is a double pole at s = 0. One is contributed by the structure and the other is from the waveform. Eq. (26) can be expanded in a manner similar to Eq. (20), and upon using Cauchy's integral theorem, the time domain representation for the linear charge density becomes

$$\overline{[\rho(t)]} = -\sum_\alpha \overline{[D_\alpha]}\,\overline{[C_\alpha]}^T \frac{\overline{[V_o(s_\alpha)]}}{(s_\alpha)^2} \overline{\overline{[U(t)]}} e^{s_\alpha t}$$

$$+ \sum_\alpha \overline{[D_\alpha]}\,\overline{[C_\alpha]}^T \frac{\overline{[V_o(0)]}}{s_\alpha^2} \overline{\overline{[U(t)]}}$$

$$+ t\sum_\alpha \overline{[D_\alpha]}\,\overline{[C_\alpha]}^T \frac{\overline{[V_o(0)]}}{s_\alpha} \overline{\overline{[U(t)]}} \tag{27}$$

Notice that the $1/s^2$ term in the frequency domain expansion has contributed a term proportional to t in the time domain. Again from physical knowledge of the time response we know that the late time behavior of the charge density must approach a constant and not grow with time. Thus, it is seen that the last sum in Eq. (27) must be zero. It is interesting to note that this sum is almost identical to that in Eq. (24) which also sums to zero, except that the natural mode vector is different.

In order to evaluate Eq. (27), it is perhaps easier to directly calculate the static response by evaluating the integral equation at s = 0, instead of performing the summation indicated by the second term. From the final value theorem,

$$\lim_{t\to\infty} f(t) = \lim_{s\to 0} sF(s) \tag{28}$$

where f and F are transform pairs. Letting F(s) be the charge density for an incident unit step, Eqs. (18) and (10) give

$$\lim_{t\to\infty}[\overline{\rho(t)}] = \lim_{s\to 0} s\left\{-\frac{1}{s}\frac{d}{dz}\,\overline{\overline{[Z(s)]}}^{-1}\,\frac{[\overline{V_o(s)}]}{s}\right\} \tag{29}$$

where the 1/s term in the incident field is shown explicitly. Simplifying this expression gives

$$[\overline{\rho(\infty)}] = -\lim_{s\to 0}\frac{d}{dz}\left(\frac{\overline{\overline{[Z(s)]}}^{-1}\,\overline{[V_o(s)]}}{s}\right) \tag{30}$$

This last expression is recognized to be the s = 0 response of the charge on the wire due to a delta-function incident field. Since $V_o(s)$ is well behaved at s = 0, it can be removed from the limiting process. Substituting Eq. (30) into Eq. (27) yields the final equation for the step response of the charge density as:

$$[\overline{\rho(t)}] = -\sum_{\alpha}[\overline{D_\alpha}]\,[\overline{C_\alpha}]^T\,\frac{[\overline{V_o(s_\alpha)}]}{s_\alpha^2}\,\overline{\overline{[U(t)]}}\,e^{s_\alpha t} - \lim_{s\to 0}\left(\frac{d}{dz}\,\frac{\overline{\overline{[Z(s)]}}^{-1}}{s}\right)\overline{[V_o(0)]} \tag{31}$$

From this relation and the corresponding equation for the wire current (Eq. (25)), it can be seen that by specifying only the pole locations $s_\alpha$ and the corresponding coupling vectors $\overline{[C_\alpha]}$, the step-wave time response for the thin-wire can be calculated. Since the only dependence on $\theta$ (the angle of incidence of the incoming pulse) occurs in the forcing vector $\overline{[V_o(s_\alpha)]}$ and the Heaviside matrix $\overline{\overline{[U(t)]}}$, the problem can be solved for many different angles of incidence without recalculating the $s_\alpha$ and $\overline{[C_\alpha]}$. Moreover, these quantities define the delta function time response of

the system. The more general time response due to an arbitrarily time varying incident field can be obtained through application of convolution or transfer function techniques.

In Eqs. (25) and (31), the product $[\overline{C_\alpha}]^T[\overline{V_o(s_\alpha)}]$ occurs. This is basically the scalar product of the coupling vector and the incident field vector. Baum[1] defines this as the coupling coefficient $c_\alpha$ at the pole $s = s_\alpha$, so

$$c_\alpha = [\overline{C_\alpha}]^T[\overline{V_o(s_\alpha)}] \quad . \tag{32}$$

Although the coupling vector is independent of the angle of incidence of the field, it is clear that $c_\alpha$ is not. From Eqs. (25) and (31), it is seen that the coupling coefficient defines how much of each mode should be used in obtaining the time domain response of the scattering wire.

It should be pointed out that this is basically the Type 4 coupling coefficient defined by Baum. Three other types of coefficients can be defined, but this last type appears to be a natural choice for the present problem.

In a practical application of this method, it is not possible to consider all of the poles in the complex s plane. As will be seen in the next section, some poles contribute more to the time response than others, since they are not so heavily damped in time. Thus the infinite sums in Eqs. (25) and (31) may be truncated when the time response appears to have converged. For the thin-wire case, only about 10 poles (plus their complex conjugates) are needed for a reasonably accurate description of the early time response. For the late time response ($ct/L > 3$) much fewer poles are needed.

## III. The Numerical Determination of the Natural Frequencies

In order to determine the natural frequencies, the coupling vectors and the natural modes for the thin-wire, it is necessary to solve the Pocklington equation as presented in Eq. (1) for a general complex frequency s. As previously mentioned, the method of moments is employed, with the basic functions chosen to be pulses and the testing functions being delta functions. Clearly, a more refined choice can be made if desired. Throughout the study, the number of unknowns, n , which describe the current have been chosen so that $n = 10 \times |s|L/\pi c$. This implies that if $s = j\omega$, ten cells per half-wavelength are used.

The location of the natural resonances of the wire are determined from Eq. (9). Regarding the determinant of the system matrix as a complex function of the frequency s, Eq. (9) can be expanded in a complex Taylor series about a point $s_o$ as

$$\Delta(s_\alpha) = 0 \approx \Delta(s_o) + \Delta'(s_o)(s_\alpha - s_o) + \frac{\Delta''}{2}(s_\alpha - s_o)^2 + \cdots \quad (33)$$

Keeping the first two terms in the expansion gives

$$(s_\alpha - s_o) \approx -\Delta(s_o)/\Delta'(s_o) \ , \quad (34)$$

which can be used to find the pole location $s_\alpha$ in an iterative manner, similar to the Newton-Raphson method for real functions. To start the solution, an initial guess of the resonant frequency must be made. From Figure 2, it is seen that the resonances appear to occur with $(\omega L/c) \approx m\pi$. From the widths of the resonance curves, an estimate of the imaginary part of (sL/c) can be made, much in the same manner as in circuit theory. Once an initial guess as to the pole location is made, Eq. (34) may be used to iteratively find the pole location.

The results of a numerical search in the complex s plane for the zeros of $\Delta(s)$ are shown in Figure 4. The ratio d/L = .01 for

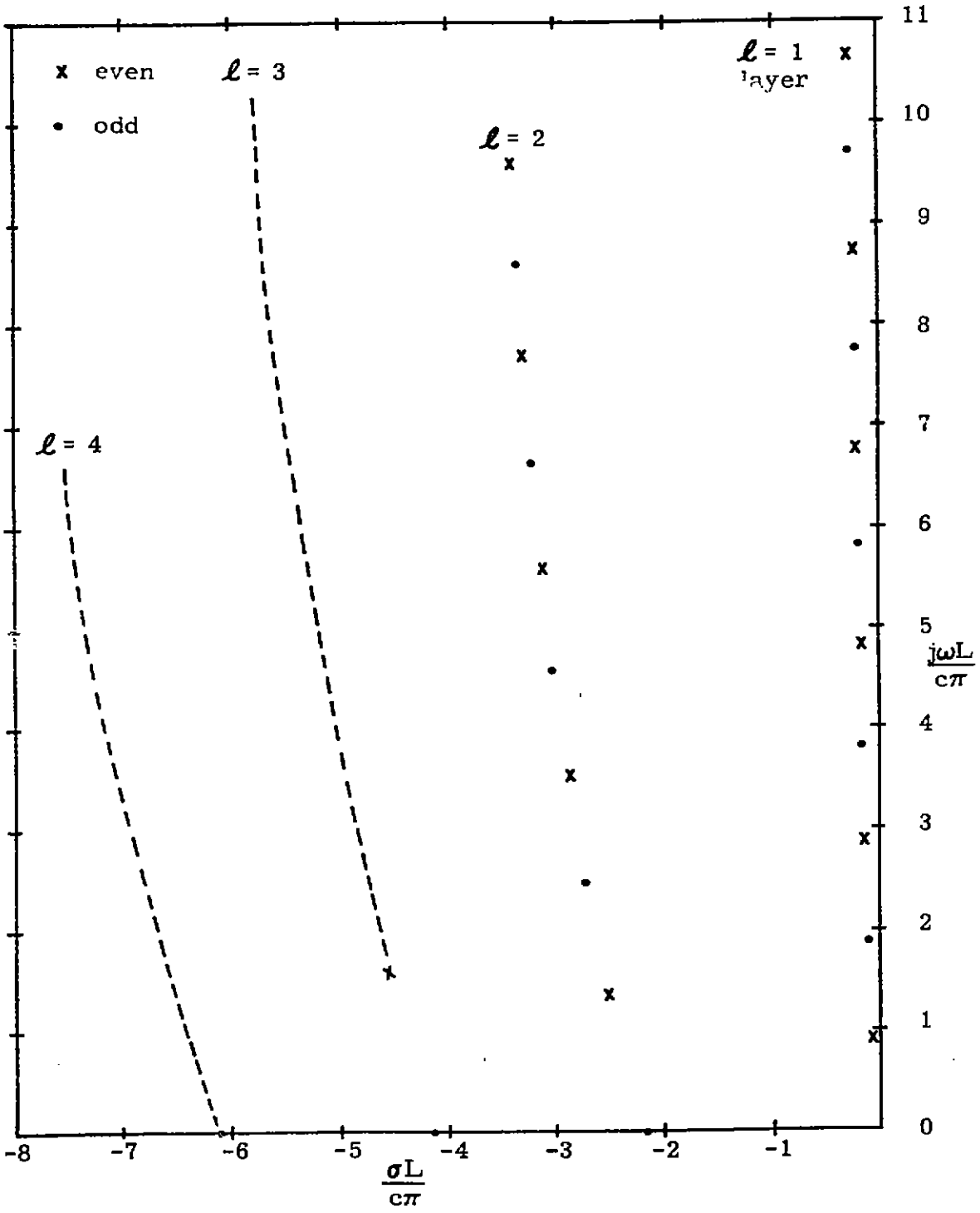


Figure 4. Pole locations in the complex frequency plane for the thin-wire of d/L = .01.

this particular thin-wire scatterer. Note that only the upper left-hand quadrant of the complex s plane is presented. As previously mentioned, only the left half of the s plane has singularities and these singularities are symmetric about the $s = \sigma$ axis. Both of these facts have been verified numerically.

It is interesting to observe the nature of these natural resonances, which appear to occur in layers. The dotted extensions of the higher order layers of poles have not been calculated, but are postulated to exist by analogy to other related problems, such as the natural resonances of the sphere. In Figure 4, the natural frequencies are presented as having mode distributions that are either symmetric or anti-symmetric with respect to the center of the scatterer. A discussion of this point will be made in the next section.

From the location of the poles in the s plane, it is noted that the single index $\alpha$ is not convenient for distinguishing between the different poles. For the present problem, the poles will henceforth be labeled by two indices as $s_{\ell,n}$, where $\ell$ refers to the layer of the pole and n refers to the pole within that layer. It will be assumed that the index n runs from 1 to $\infty$ and in doing so, both of the complex conjugate roots are considered for a particular n, if $s_{\ell n}$ is complex.

As the solution I(s) is evaluated along the axis $s = j\omega$, it is obvious that the first layer of poles contributes the most effect, as is evident in Figure 2. The effects of the other layers of poles are not so obvious. In the time domain, it is noted that the effects of the poles with a large value of $\sigma$ die out rapidly as they are heavily damped.

A similar problem has been worked out for the scattering by a sphere.[1,10] For that problem, there are two sets of poles, one for the electric modes and the other for the magnetic modes and are determined by the zeros of $[(-is)h_n^{(2)}(-is)]' = 0$ and $(-is)h_n^{(2)}(-is) = 0$ respectively. The locations of these poles are

shown in Figures 5 and 6. The electric modes of the sphere correspond most closely to the natural modes on the thin-wire, since there is a charge density associated with each mode. For the magnetic modes which are divergenceless, no charge density occurs and these are not found in the thin-wire solution.

In comparing Figures 4 and 6, it is seen that there is a similarity in the pole patterns in the s plane. The first layer of poles for the sphere is farther away from the $j\omega$ axis than for the thin-wire, indicating that the sphere has a lower Q than the wire. This result is also observed as the wire radius becomes larger. Figure 7 shows the trajectories of the first 7 poles of the $\ell = 1$ layer as the ratio d/L varies. As d/L increases, these poles move farther away from the $j\omega$ axis.

More expanded views of the trajectories of the first three poles as d/L is varied are presented in Figures 8, 9 and 10. For the first resonance (n = 1), the approximate locations as determined theoretically by S. W. Lee[5] have also been shown. For thin wires, the agreement is reasonably good, but deteriorates as d/L increases.

Some numerical difficulties were obtained in attempting to find the higher-order natural resonances for the thicker wires. As the wire diameter becomes bigger, the system matrix for the E-field formulation becomes ill-conditioned and substantial numerical errors are found in its inverse. As a result, the pole locations are also in error. For thicker wires, the H-field integral equation should provide a better starting point for the analysis.

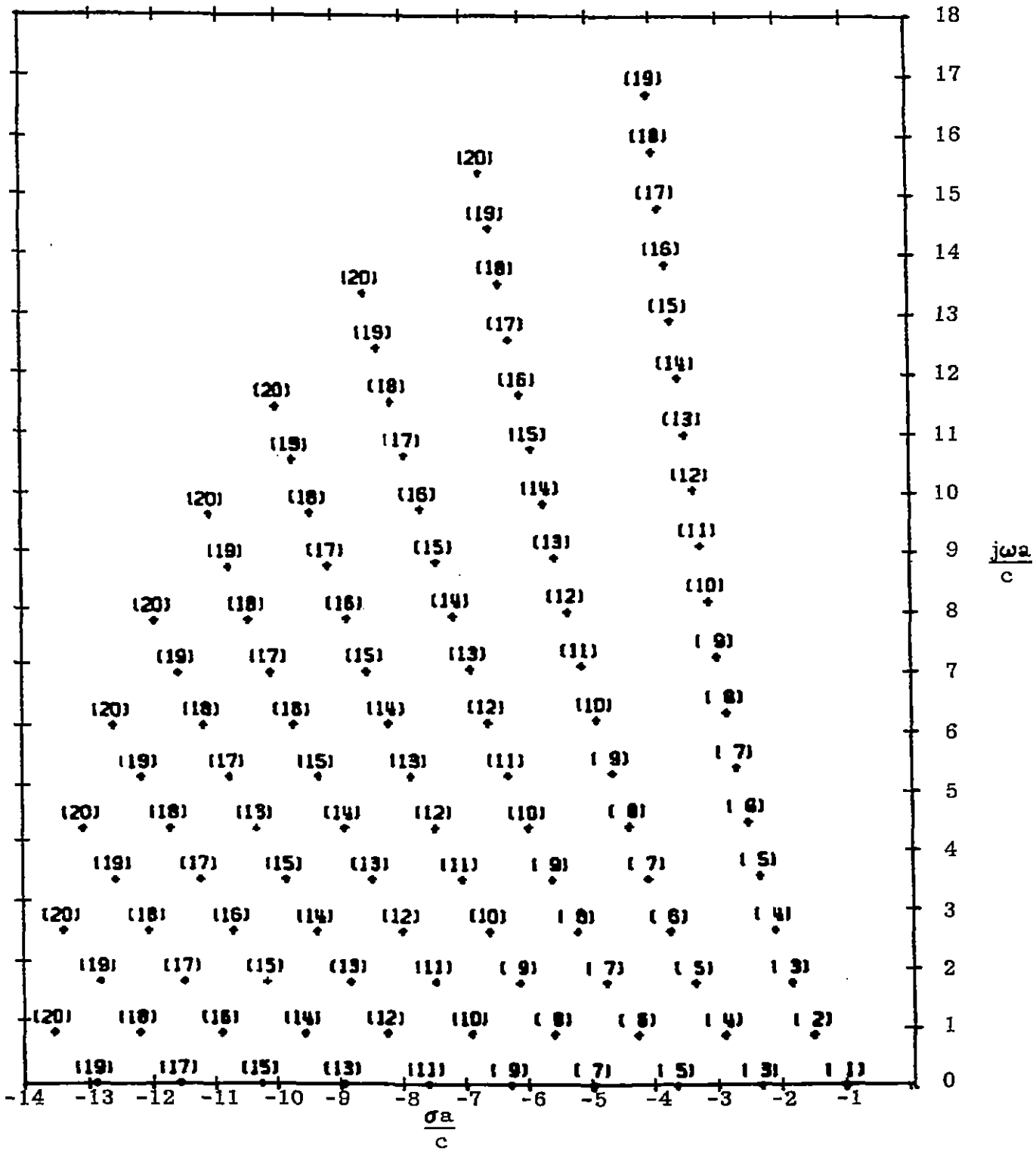


Figure 5. Pole locations for the magnetic modes of a perfectly conducting sphere. The number in brackets indicates the order of the Hankel function.

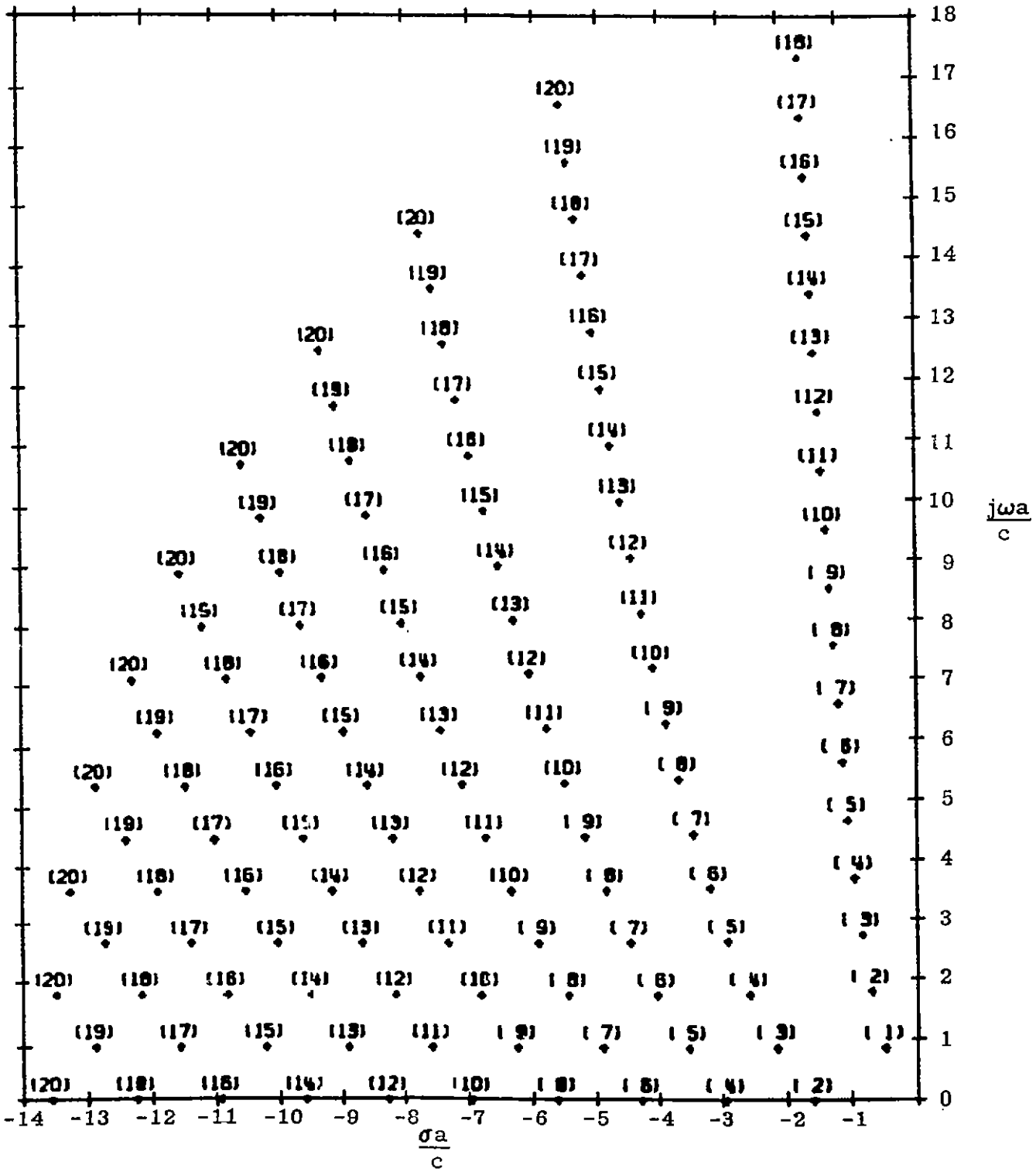


Figure 6. Pole locations for the electric modes of a perfectly conducting sphere. The number in brackets indicates the order of the Hankel function.

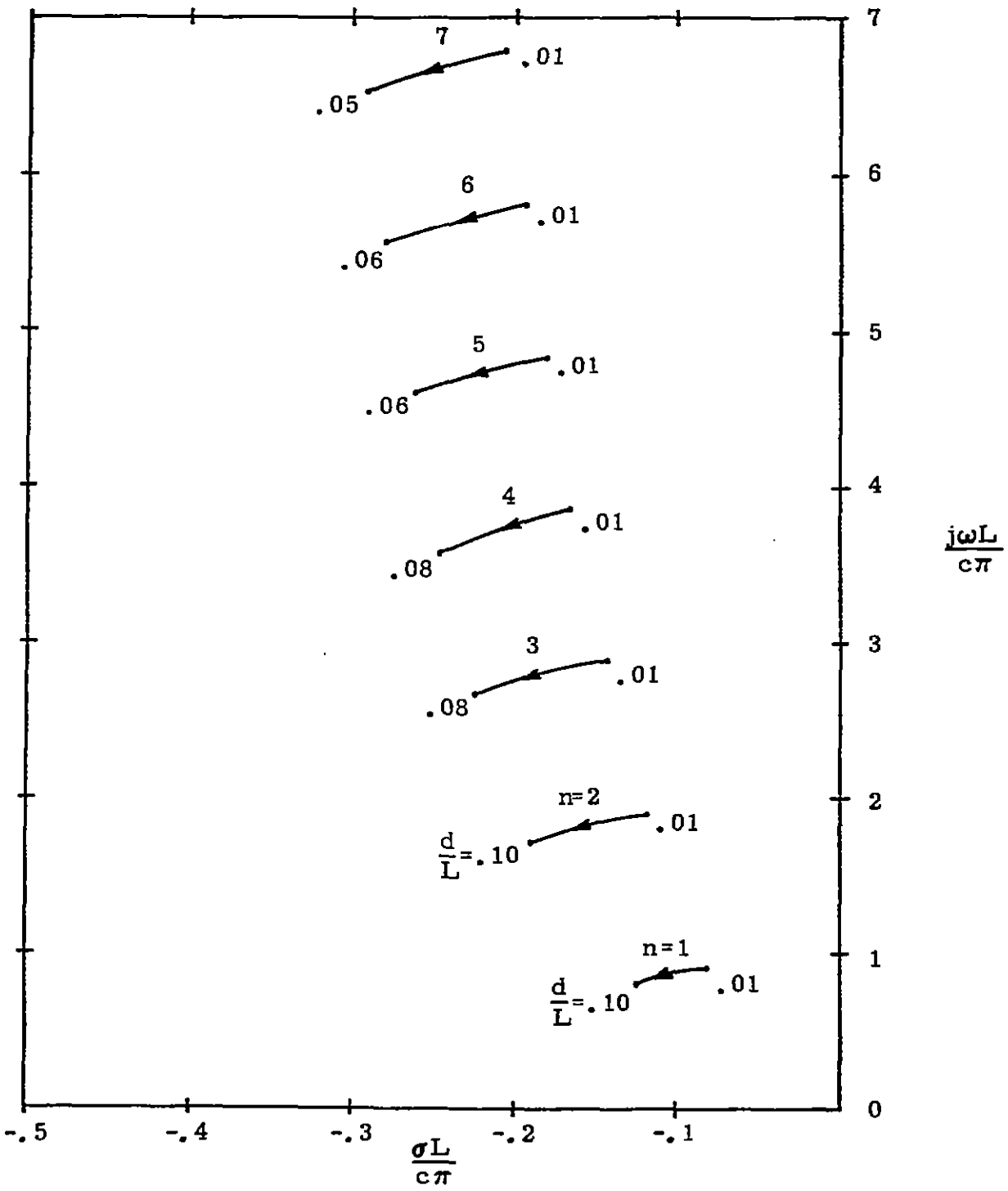


Figure 7. Plots of the trajectories of the first seven poles for the thin-wire as d/L is increased from .01.

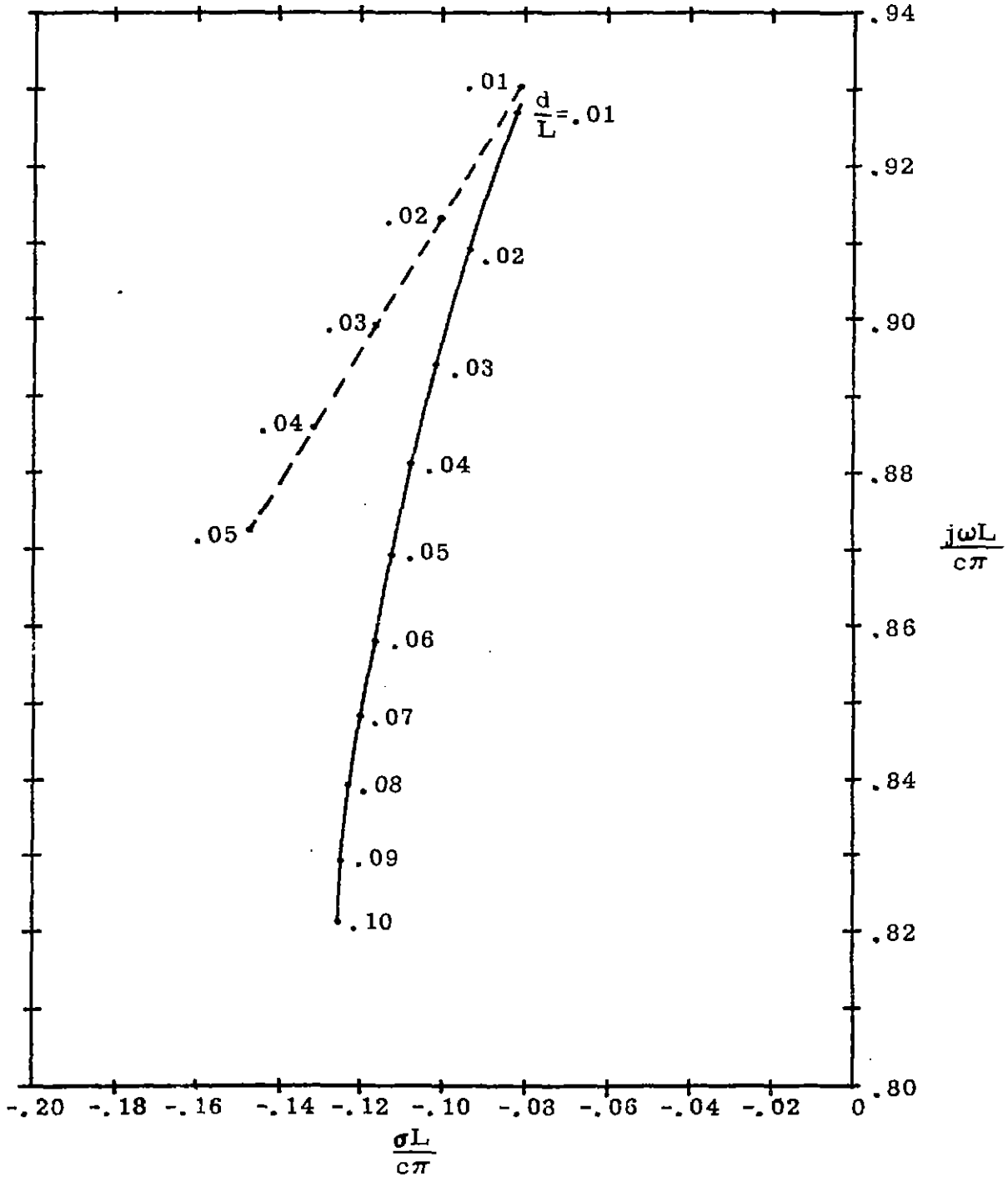


Figure 8. The trajectory of the first pole n=1, $\ell$=1 as a function of the ratio d/L. The dotted line is the approximate pole location from Lee and Leung.

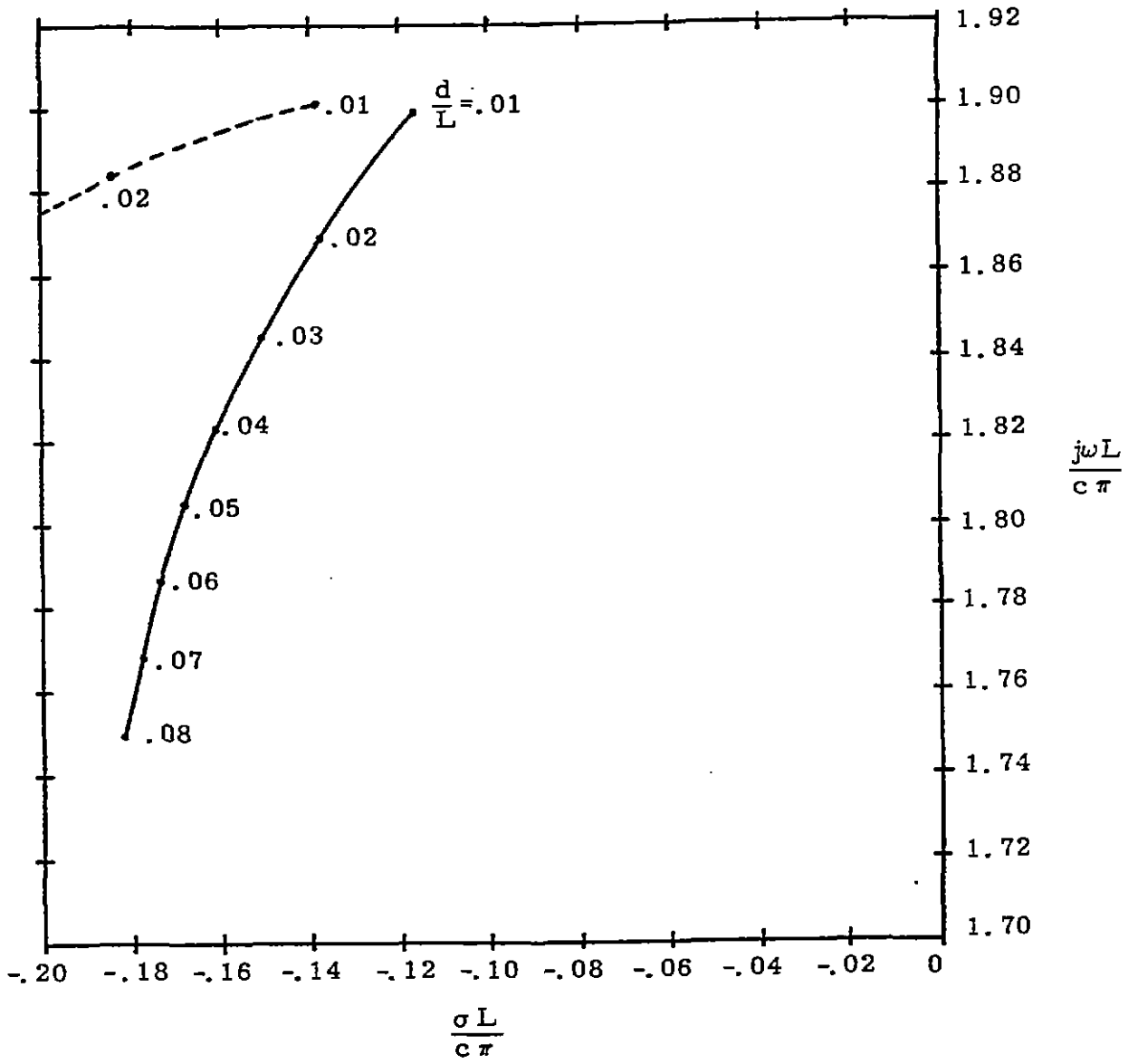


Figure 9. The trajectory of the second pole n=2, $\ell$=1 as a function of the ratio d/L. The dotted line is from Lee and Leung.

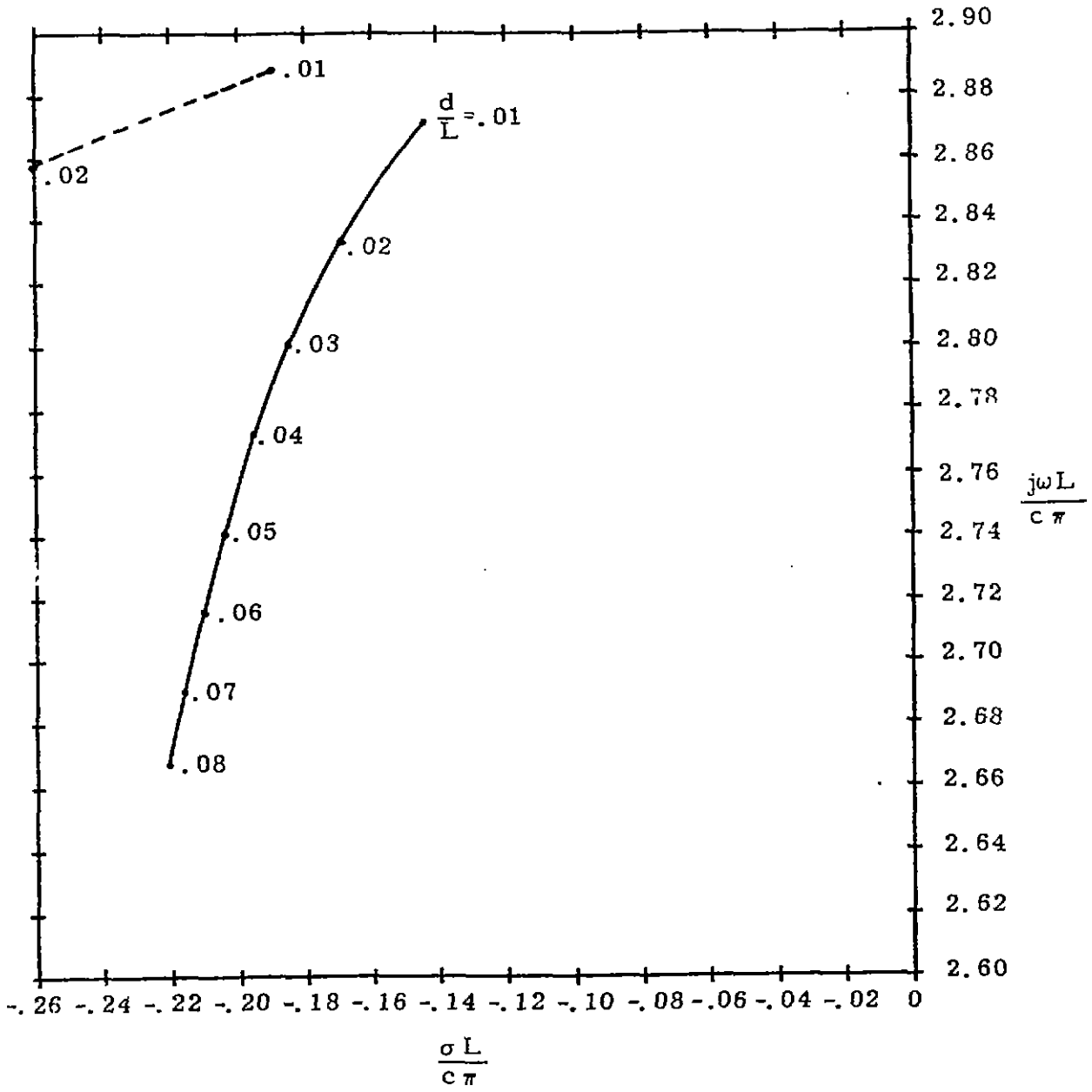


Figure 10. The trajectory of the third pole n=3, $\ell$=1 as a function of the ratio d/L. The dotted line is from Lee and Leung.

## IV. Evaluation of the Residue Matrix

Once the pole locations have been determined, it becomes necessary to evaluate the system residue matrix at each pole as defined by Eq. (12). Suppose the residue at the $k^{th}$ pole is desired. As seen from Eq. (12) the inverted system matrix $\overline{\overline{[Z(s)]}}^{-1}$ becomes undefined as s approaches $s_k$. Multiplying both sides of Eq. (12) by $s - s_k$ and taking the limit gives

$$\lim_{s \to s_k} (s - s_k) \overline{\overline{[Z(s)]}}^{-1} = \lim (s - s_k) \sum_{\alpha} \frac{\overline{[R_\alpha]}}{s - s_\alpha} = \overline{[R_k]} \qquad (35)$$

Denoting the difference between the frequency s and the pole frequency $s_k$ by $\varepsilon$ so that $s = s_k + \varepsilon$ gives Eq. (35) in the following form

$$\overline{[R_k]} = \lim_{\varepsilon \to 0} \varepsilon \overline{\overline{[Z(s_k + \varepsilon)]}}^{-1} . \qquad (36)$$

The numerical method for finding $\overline{[R_k]}$ is to evaluate Eq. (36) with a suitably small value of $\varepsilon$ such that the residue matrix does not vary as $\varepsilon$ is changed.

As previously mentioned the residue matrix may be defined as the outer product of two vectors, and for the electric field formulation, these vectors are identical. The vector $\overline{[C_\alpha]}_o$ is the solution to the equation

$$\overline{\overline{[Z(s_\alpha)]}}\, \overline{[C_\alpha]}_o = 0 \qquad (37)$$

which is assumed to be normalized such that the maximum value of $\overline{[C_\alpha]}_o$ is real and has a value of unity. With this normalization, Eq. (16) can be written as

$$\overline{\overline{[R_\alpha]}} = \beta_\alpha \overline{[C_\alpha]}_o \overline{[C_\alpha]}_o^T \tag{38}$$

with $\beta_\alpha$ being the appropriate normalization factor.

Once the normalized solution to Eq. (37) is determined, and the residue matrix of Eq. (36) is computed, the normalization constant $\beta_\alpha$ can be found from Eq. (38).

The normalized natural modes for the first three resonances occurring in the $\ell = 1$ layer of poles are presented in Figure 11. The ratio d/L = .01 for this data. The normalizing factors $\beta_\alpha$ are also presented. It is noted that the modes are either symmetric or anti-symmetric about the midpoint of the scatterer. For these modes, it is also observed that the imaginary part is relatively small, implying that these natural modes are almost real functions of position. Whether or not these imaginary parts arise from numerical errors is a question still to be addressed. It is known from the sphere problem that the natural modes are purely real functions. This appears not to be the case for the thin-wire.

In the sphere problem, there are some poles which have the same natural mode distribution. For example, in Figure 6, the poles for n = 2 in the first branch and in the second branch both have the same natural mode. In fact, all poles with the same index n (which refers to the order of the spherical Hankel function) have the same natural mode distribution. In the thin-wire case, this would correspond to the n=2 pole in the $\ell = 1$ layer having the same mode distribution as the n = 1 pole in the $\ell = 2$ layer. Figure 12 shows that this is not the case for the thin-wire. The natural mode for $s_{1,2}$ has a maximum value closer to the center of the wire than does the mode for $s_{2,1}$. Moreover, it is known that the mode for $s_{2,1}$ is completely real, as the pole resides on the $-\sigma$ axis, whereas the other pole does have a small imaginary part as indicated in Figure 11.

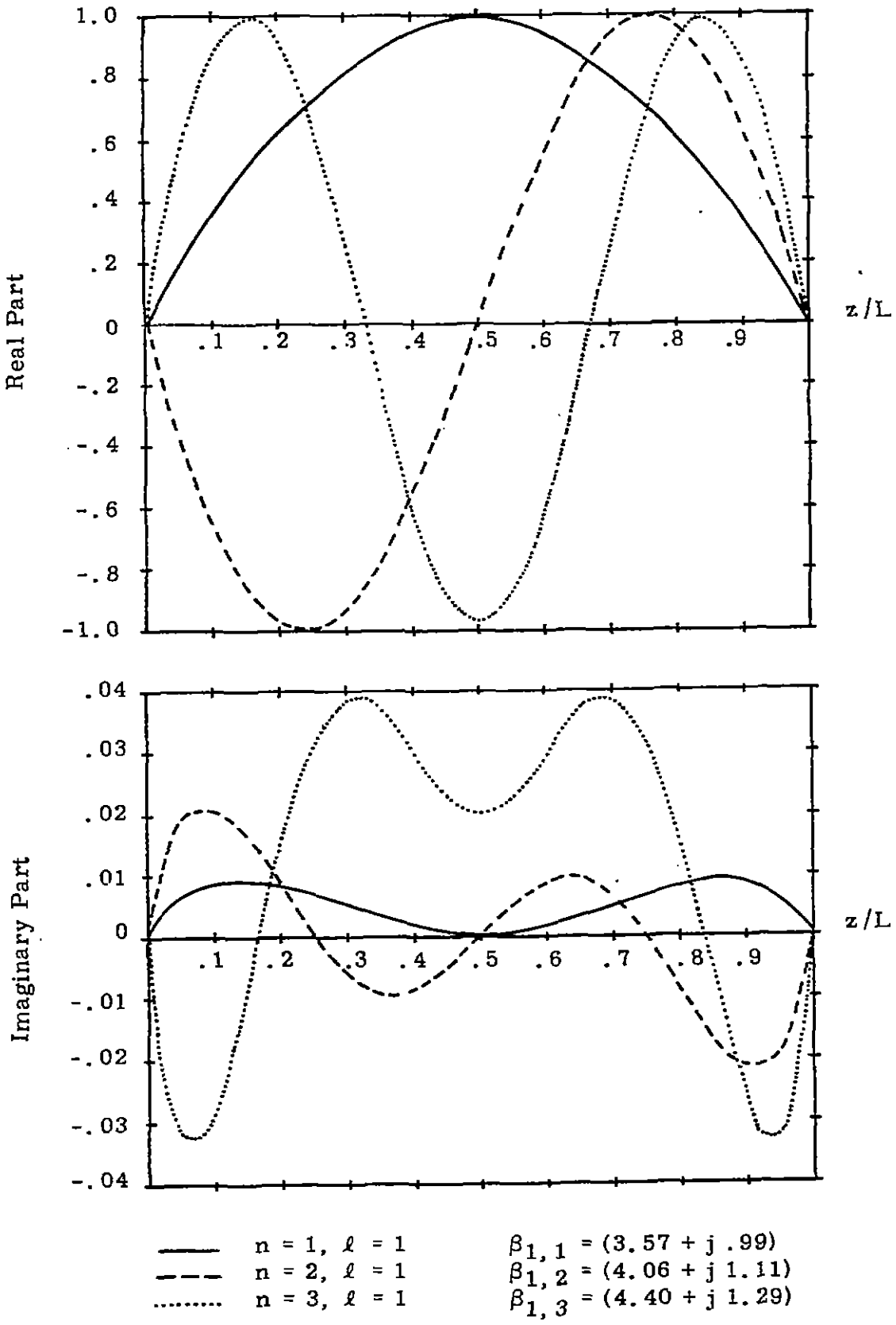


Figure 11. Plots of the real and imaginary parts of the first three normalized natural modes for the thin wire, d/L = .01.

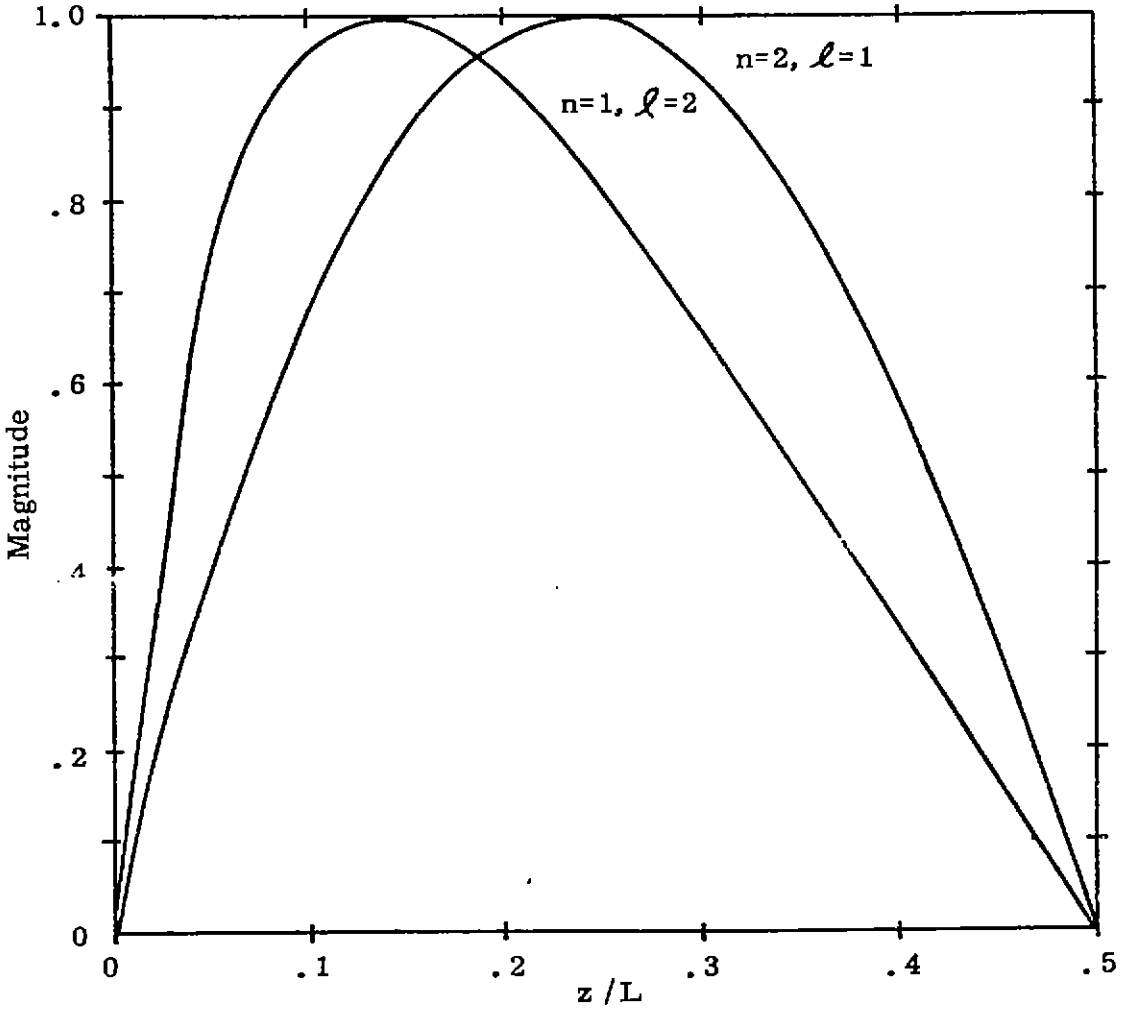


Figure 12. The normalized magnitudes of the natural modes for n=2, $\ell$=1 and n=1, $\ell$=2. In the sphere, these modes are identical.

The coupling coefficient as defined by Eq. (32) is particularly useful in attempting to reconstruct the time behavior of the currents for any angle of incidence $\theta$. Figure 13 shows the three normalized coefficients for $\ell = 1$ and $n = 1, 2, \& 3$ as a function of the angle $\theta$ for the incident field as shown in Figure 1. Note that for this normalized coupling coefficient, the coupling vector itself $[\overline{C_\alpha}]$ has been normalized to have a maximum of unity. In addition, the coupling coefficient has been multiplied by a factor $e^{-(s_\alpha L/2c)\cos\theta}$ so as to reference $t = 0$ at the midpoint of the wire and thus preserve any symmetries occurring in the coupling coefficients.

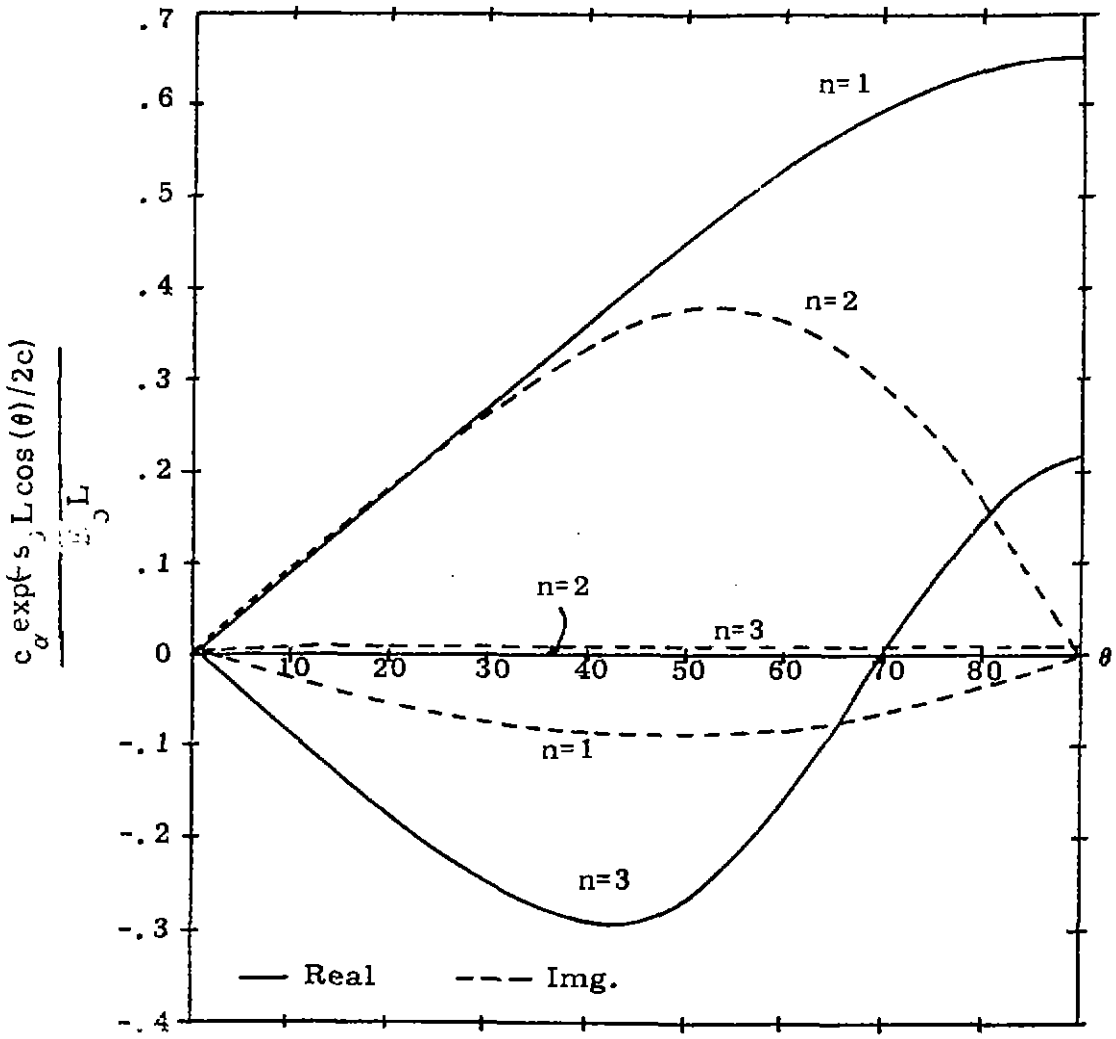


Figure 13. Plots of the coupling coefficients as a function of the angle of incidence $\theta$ for the first three poles in the $\ell = 1$ layer.

## V. The Time Domain Response

With the natural modes and resonant frequencies computed as in the previous sections, the time domain response of the currents and charges on the wire may be easily computed. From Eq. (25) it is seen that the current time response is a sum over the various poles which contribute to the response. The coupling and mode vector $[\overline{C_\alpha}]$ and the pole location $s_\alpha$ are independent of the angle of incidence, $\theta$, of the incoming wave. Hence, once these values are calculated and stored, any angle of incidence can be easily considered by evaluating $[\overline{V_o(s_\alpha)}]$ and $[\overline{\overline{U(t)}}]$ for the particular value of $\theta$.

The case of $\theta = 30°$ is considered in Figures 14a through 14d, where the currents at $z/L = .25$, $.50$ and $.75$ are plotted as functions of time. As before, $d/L = .01$. These curves show the convergence of the time response as the number of poles is increased. Only poles for the $\ell = 1$ layer have been included, as it was observed that the $\ell \geq 2$ layers gave a negligible contribution to the current response. In these curves it is interesting to note that for n being even, there is no contribution to the current of $z/L = .50$. That this should be correct may be verified from the fact that the natural mode vector for even n is an odd function about the wire middle, and hence gives zero contribution at that point. It should also be noted that for $n = 4, 8$, etc., there are zero contributions to the current at all three points. This can be also verified by looking at the magnitude of $I(j\omega)$ in Figure 2, where it is seen that the contributions of the $4^{th}$ and $8^{th}$ poles are zero.

The resultant curves after 10 poles have been considered appear to have converged quite well, even for early times. The effects of causality are clearly indicated. A comparison of these results to those obtained by solving the integral equation along the $j\omega$ axis and taking a Fourier transform (Figure 15) shows that the agreement between the two methods is excellent. For the Fourier transform results, a spectrum from $kL = 0$ to $kL = 40$ was

used, and the integral equation was evaluated at 128 unique frequency points. For the natural resonance method, only 10 inversions of the integral equation are required, in addition to the search for the poles. Typical computation times on a CDC 6600 were 150 sec. for the natural resonance method vs. 400 sec. for the Fourier transform method.

As may be seen from the current curves, the late time ($ct/L \geq 3$) behavior is fairly well defined after the first 4 or 5 poles have been considered. If one wishes to average out the ripples in the early time portions of the curves, it could be that only 6 poles are needed for this particular case.

Similar convergence behavior was noted for the linear charge density at $z/L = 0$ and 1.0. The curves in Figure 16 show the normalized charge density $\sigma/(\varepsilon_o E_o L)$ as a function of time for both methods of computation. The early time behavior of the charge for the natural resonance method is not as smooth as in the other curves, but nevertheless, the agreement between the two is very good.

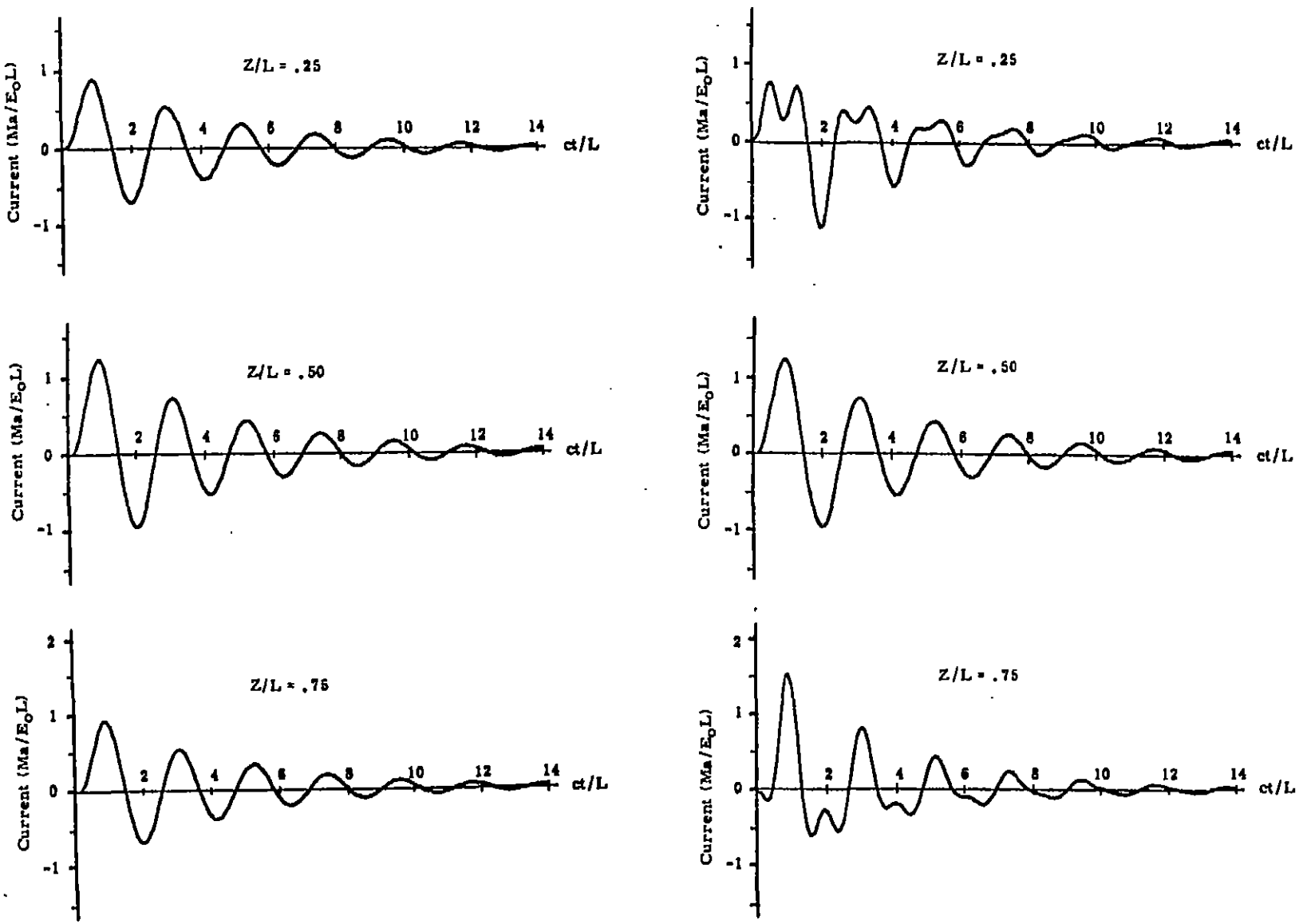


Figure 14a. Plots of the time response of the current at three points on the scattering wire, shown as a function of the number poles. The angle of incidence is $\theta$=30°, and d/L=.01. Only the $\ell$=1 poles are considered.

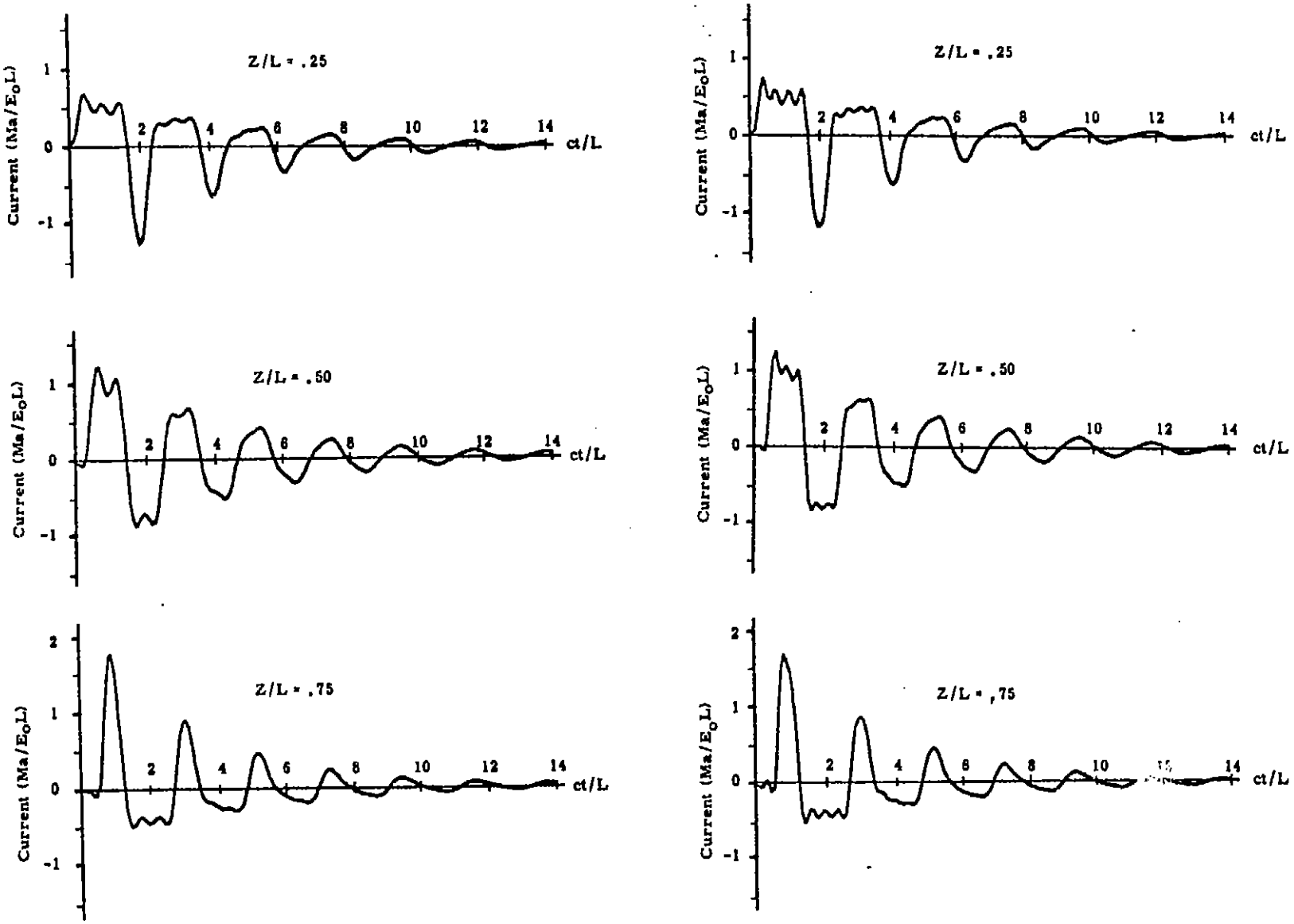


3 & 4 Poles Used

5 Poles Used

Figure 14b.

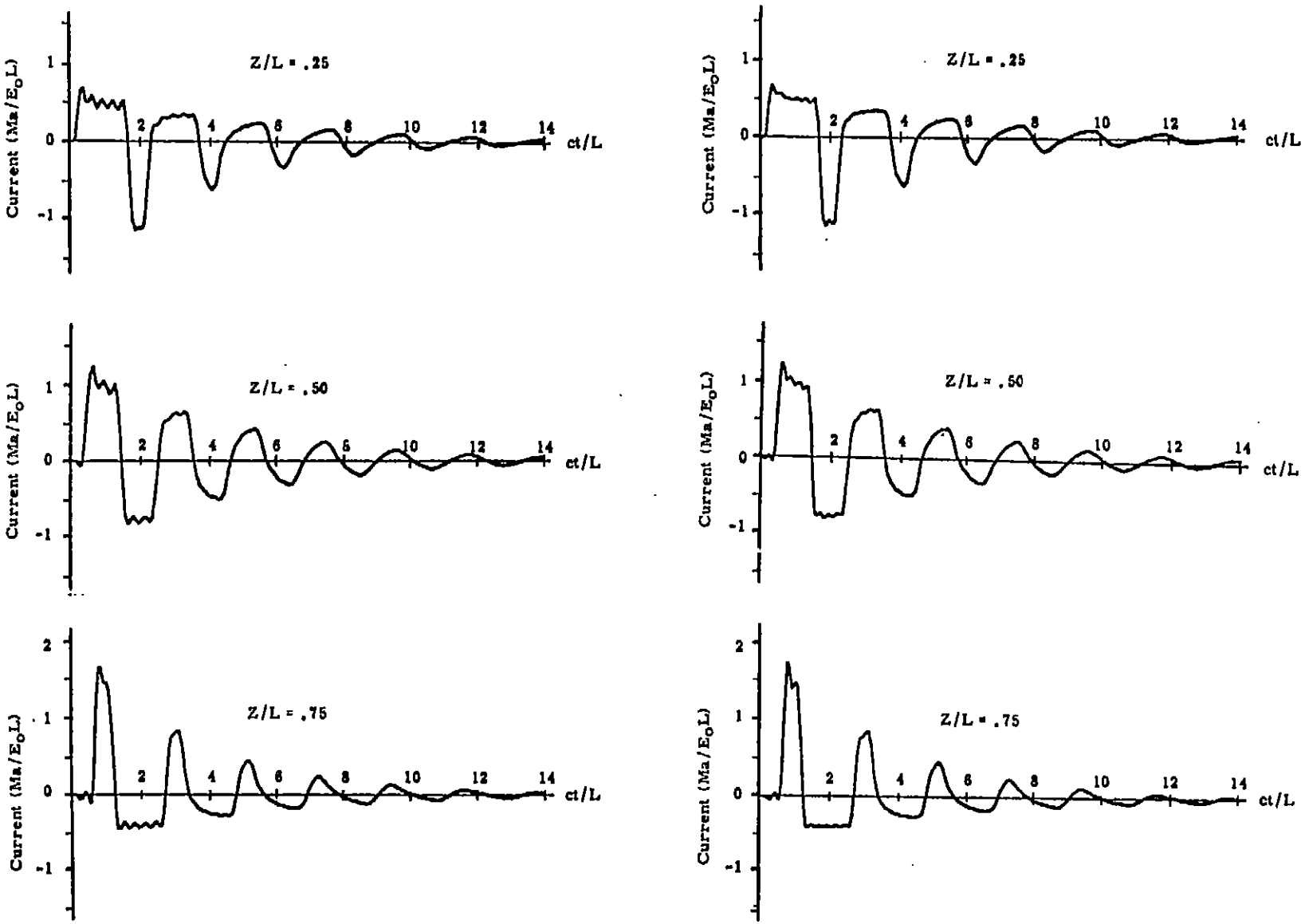


Figure 14c.

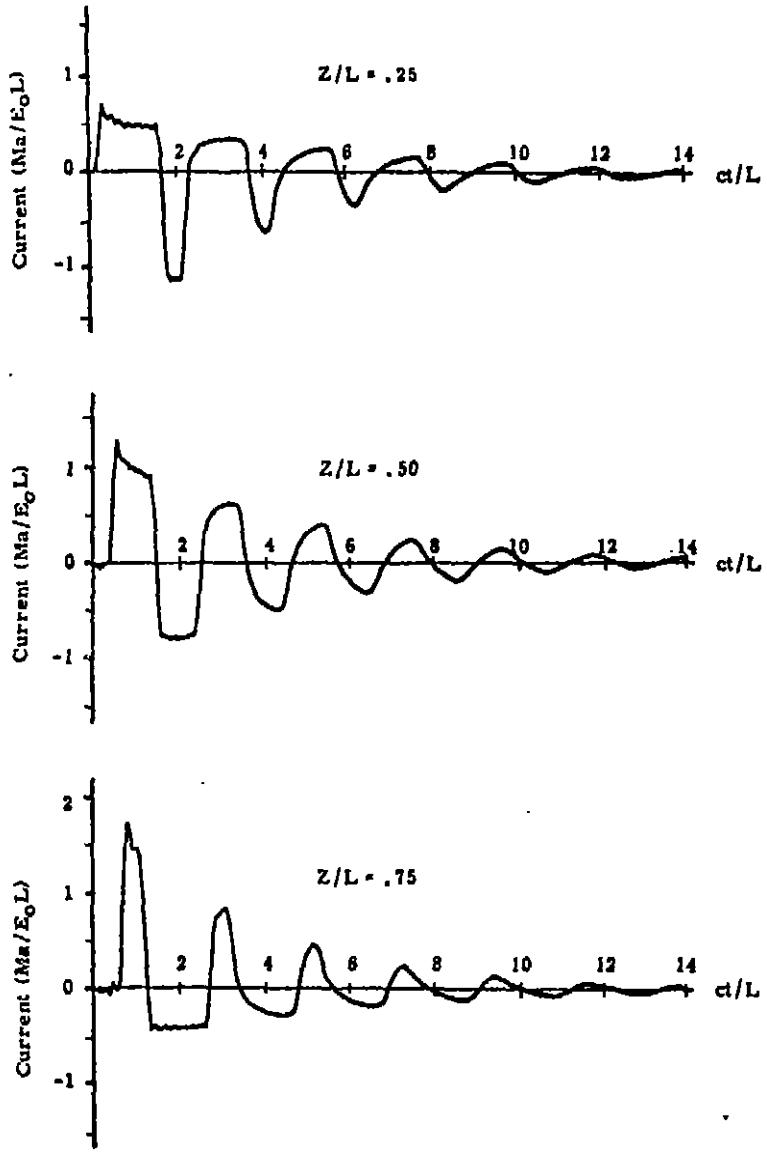


9 Poles Used

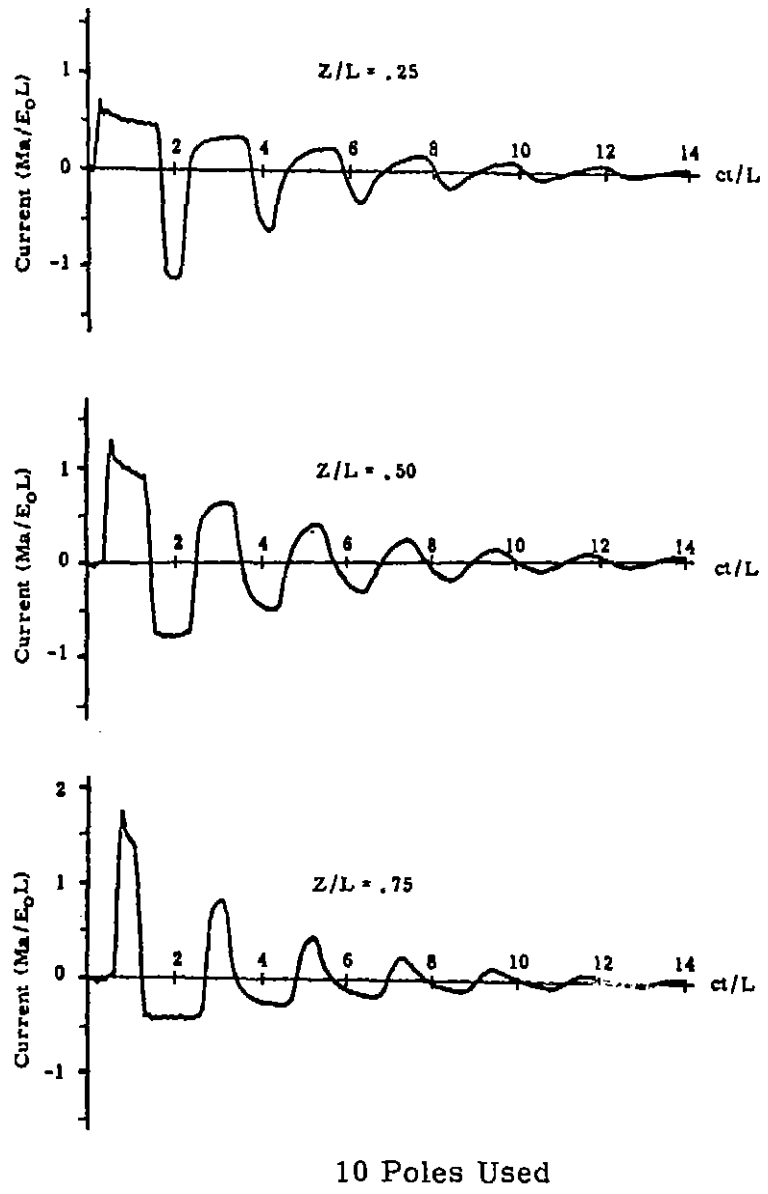


10 Poles Used

Figure 14d.

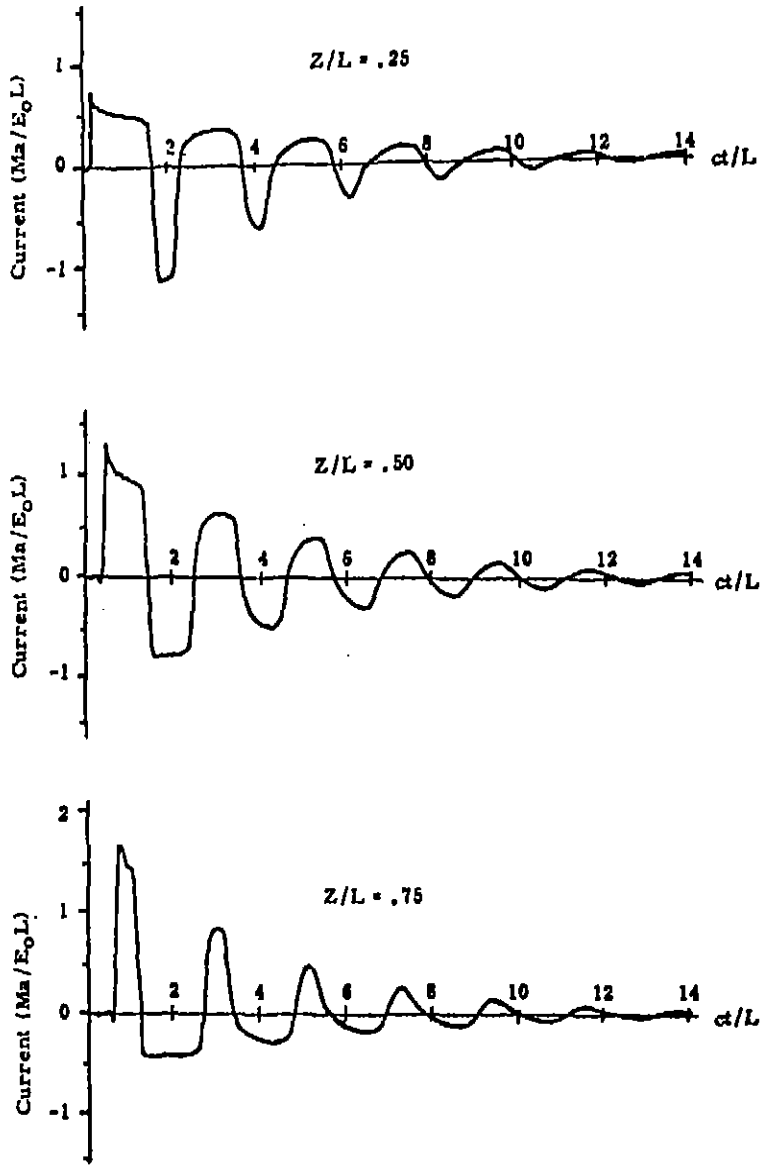


Fourier Inversion Solution

Figure 15. The time response of the currents on the scattering wire of d/L = .01 as obtained by the integral equation and Fourier inversion method. As in the previous figure, $\theta = 30°$.

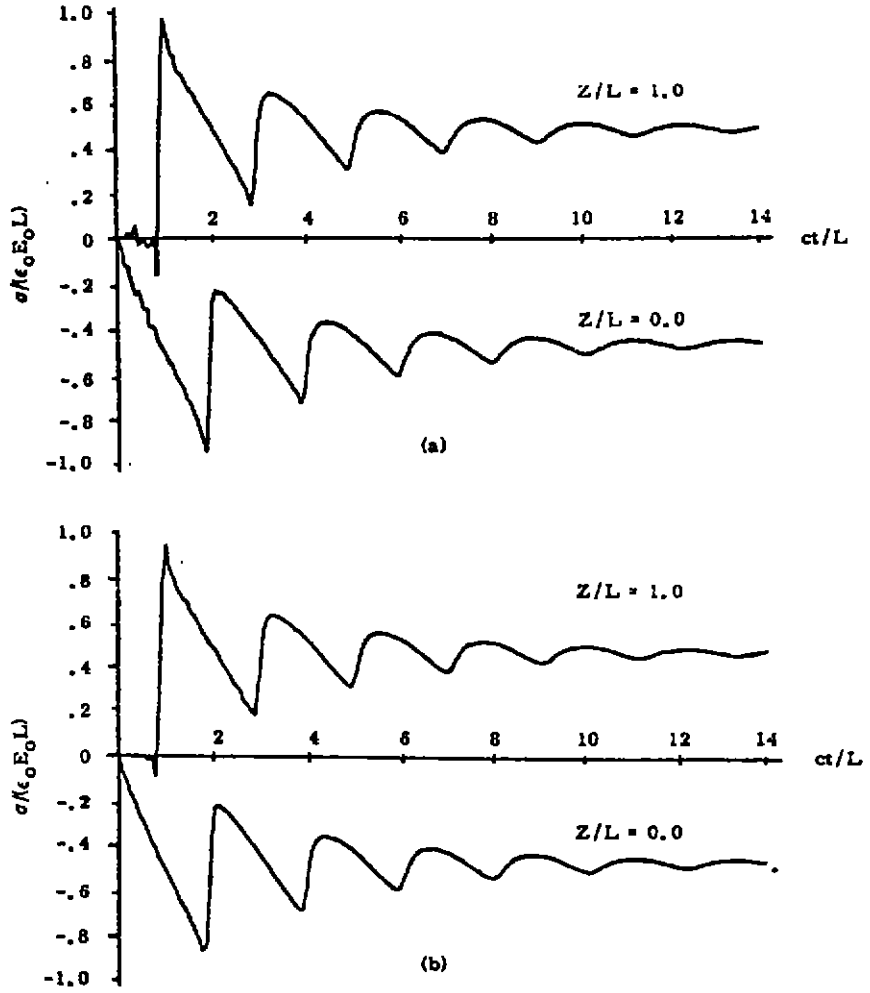


Figure 16. Plots of the linear charge density occurring at the ends of the wire with a step wave at $\theta = 30°$ incident. Part a shows the results for 10 poles and part b shows the results obtained by performing the Fourier inversion.

## VI. Conclusions

From the electric field integral equation formulation of the frequency domain scattering from a thin-wire, the exterior natural resonant frequencies have been computed. The coupling and natural mode vectors, as evaluated at each of the natural frequencies, were also calculated and used in obtaining the time domain behavior of the induced current on the scatterer. From this study, a number of observations can be made about this method and its application to the thin-wire. These may be summarized as follows:

1) The exterior natural resonant frequencies of the thin-wire lie in left half portion of the complex frequency plane, and exhibit conjugate symmetry about the real $\sigma$ axis.

2) The natural frequencies of the wire all have a finite real part, corresponding to damping by radiation.

3) The natural frequencies for the wire occur in layers as in the sphere, with the first layer being most important in determining the time response, due to its proximity to the $j\omega$ axis. As the thickness of the wire increases, the poles move away from the $j\omega$ axis.

4) The singularities in the current response appear to be described by simple poles.

5) For scattering bodies of finite extent, there are no branch cuts in the complex frequency plane.

6) The residue matrix at one of the natural frequencies is the outer product of the field coupling vector and the natural mode vector. For the electric field formulation, these two vectors are identical.

7) The time domain response of the structure can be computed for any angle of incidence and shape of incident waveform by knowing the coupling and mode vectors and the corresponding natural frequencies. For the late time response

(ct/L > 3) only 3 or 4 poles may be required for an adequate description of the response.

8) For times such that the wavefront has completely passed by the wire, the current response is a simple sum of damped sinusoids. For earlier times, the presence of certain regions of the wire is not felt and this must be accounted for in the determination of the response through the use of a matrix of Heaviside functions.

In the course of this work, a number of assumptions and observations have been made which leave unanswered questions regarding this method. It would be interesting if future work could address some of these questions, both from an analytical and numerical point of view.

1) Under what conditions, if any, do poles of order greater than one occur? If they do occur, how are they best treated numerically?

2) Does an antenna with a δ-source gap have a branch cut in the s plane?

3) In another note[11] a finite wire within a parallel plate region was treated in the frequency domain. Are the discontinuities observed in the response as jω is increased due to branch cuts in the s plane?

4) Can the problem in 3) above be treated by the natural resonance method?

5) Are the natural modes, in general, real functions of position along the wire, or are they complex?

6) Can the method be successfully applied to more complex bodies such as crossed wires?

7) Can it be shown rigorously that the essential singularities at infinity of the inverted system matrix are not required to find the time domain response? Stated in other terms, can it be shown analytically that the

integral at infinity in the application of the residue theorem can be neglected?

Answers to these questions will aid in a better understanding of this method, and will facilitate its usage on a wider basis for the description of electromagnetic scattering and antenna problems.

## References


1. Baum, C. E., "On the Singularity Expansion Method for the Solution of Electromagnetic Interaction Problems," *EMP Interaction Note-88*, December 1971.
2. Brigham, E. O., and Morrow, R. E., "The Fast Fourier Transform," *IEEE Spectrum*, December 1967, pp. 63-70.
3. Cooley, J. W., and Tukey, J. W., "An Algorithm for the Machine Calculation of Complex Fourier Series," *Math. Comput.*, vol. 19, April 1965, pp. 297-301.
4. Harrington, R. F., *Field Computation by Moment Methods*, Mac Millan, 1968.
5. Lee, S. W., and Leung, B., "The Natural Resonance Frequency of a Thin Cylinder and its Application to EMP Studies," *EMP Interaction Note 96*, February 1972.
6. Marin, L., and Latham, R. W., "Analytical Properties of the Field Scattered by a Perfectly Conducting, Finite Body," *EMP Interaction Note 92*, January 1972.
7. Mei, K. K., "On the Integral Equations of Thin-Wire Antennas," *IEEE Trans. on Antennas and Prop.*, May 1965, p. 374.
8. Page, L., and Adams, N., "The Electrical Oscillations of a Prolate Spheroid, Paper I," *Phys. Rev.*, vol. 33, 1938, pp. 819-831.
   Page, L., "The Electrical Oscillations of a Prolate Spheroid, Paper II, Prolate Spheroidal Wave Functions," *Phys. Rev.*, vol. 65, nos. 3 and 4, pp. 98-110.
   Page, L., "The Electrical Oscillations of a Prolate Spheroid, Paper III, The Antenna Problem," *Phys. Rev.*, vol. 65, nos. 3 and 4, pp. 111-117.
9. Pocklington, H. C., "Electrical Oscillations in Wires," *Proc. of the Cambridge Philosophical Society*, 1897, pp. 324-332.
10. Stratton, J. A., *Electromagnetic Theory*, McGraw Hill, 1941.
11. Tesche, F. M., "On the Behavior of Thin-Wire Scatterers and Antennas Arbitrarily Located Within a Parallel Plate Region, I (The Formulation)," *EMP Sensor and Simulation Note 135*, August 1971.